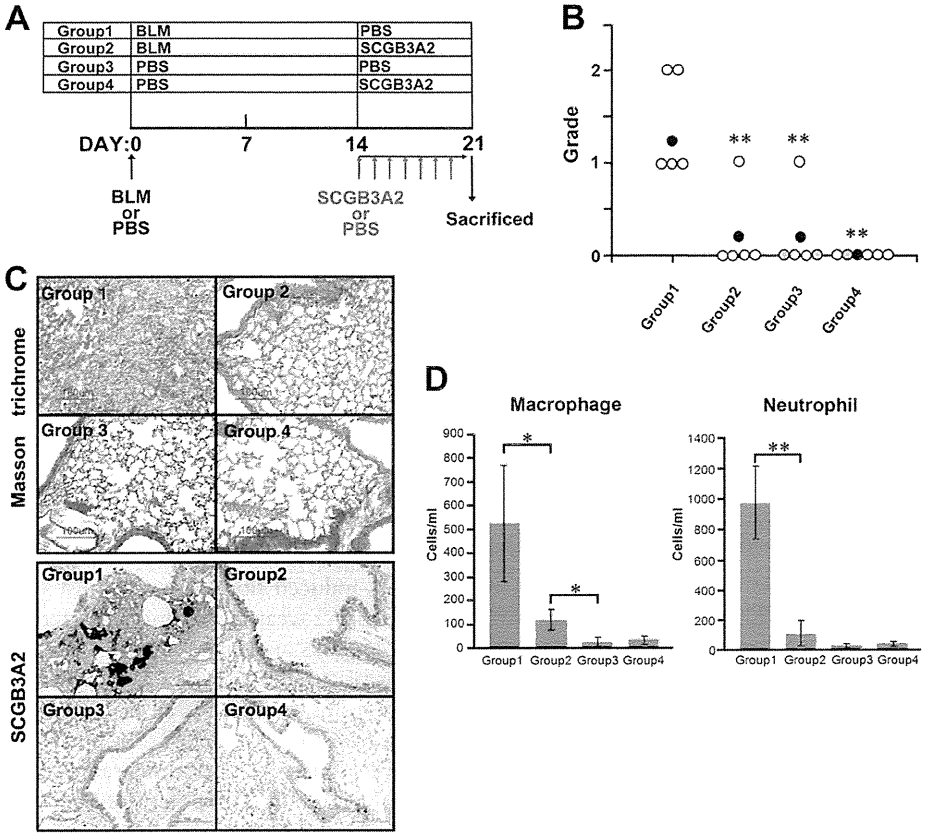

FIGURE 4. **Inhibition of BLM-induced lung fibrosis by SCGB3A2.** *A*, shown is a scheme to prepare BLM-induced fibrosis model mice. BLM or PBS was administered to the lungs of C57BL/6N mice by intratracheal intubation at day 0. SCGB3A2 or PBS was administered to mice by intravenous injection once daily for a week starting at day 14 followed by euthanasia at day 21. The four groups of mice were subjected to the studies as shown. PBS was administered as a control in Groups 3 and 4. Whole experiments were carried out at least twice. *B*, grading of fibrosis carried out as described under "Experimental Procedures." BLM administration resulted in production of fibrous tissue, focally or diffusely in lungs of Group 1, whereas no fibrous tissue formation was observed in four of five lungs exposed to BLM followed by SCGB3A2 treatment in Group 2. *White circle*, no lesions; *black circle*, mean ($n = 5$); *gray*, presence of a few infiltrating foci of lymphocytes or very small granulomas. **, $p < 0.01$, Group 1 *versus* Groups 2, 3, or 4. *C*, Masson's Trichrome staining and immunohistochemistry for SCGB3A2 are shown. Collagen fibers were focally detected as a blue color by Masson trichrome staining in the parenchyma of the lungs of mice in Group 1 but not the lungs of other groups. Excessive SCGB3A2 expression was found in a part of the epithelial cells and in the foci of fibrosis as a brown color by immunohistochemistry in Group 1. Representative staining is shown ($n = 5$). *D*, shown are the number of macrophages and neutrophils in BALF. The number of macrophages and neutrophils increased by BLM (*Group 1*) was significantly decreased by administration of SCGB3A2 (*Group 2*), especially neutrophils which reduced to the levels of control (*Group 3* and *Group 4*). The graph shows the mean ± S.D. from 5 lungs per group ($n = 5$). *, $p < 0.05$; **, $p < 0.01$.

ular transducer activity" categorized by only one term "Molecular Function" were up-regulated by short-term treatment of SCGB3A2 (Table 3). The TGFβ signaling was among the top pathways identified by the Pathway Mapping program (Fig. 5), further supporting our conclusion that SCGB3A2 affects the TGFβ signaling pathway.

Further analysis revealed that the expression of matrix metalloproteinases (MMPs) and other extracellular matrix (ECM)-degrading enzymes that degrade damaged tissues as well as enzymes synthesizing collagen I, fibronectin, hyaluronic acid, and other components of wound provisional ECM was altered after BLM and/or SCGB3A2 treatment (supplemental Table S2). qRT-PCR was performed to confirm the alterations of gene expression in BLM-treated lungs with (Group 2) and without (Group 1) SCGB3A2 (Fig. 6). High levels of MMP2, MMP12, and MMP14 expression in BLM-treated lungs (Group 1) were significantly decreased by the administration of SCGB3A2 (Group 2); in particular, MMP14 returned to the levels of the "no BLM treatment" groups (Group 3 and 4). Cathepsin S and D that belong to a group of proteinases were also highly expressed in BLM-treated group (Group 1), and decreased to a level similar to control by SCGB3A2 (Group 2). Cathepsin C levels did not show any statistically significant difference among the four groups of mice. These data further indicated a role for SCGB3A2 in suppression of lung fibrosis induced by BLM.

DISCUSSION

This study revealed that SCGB3A2 possesses anti-fibrotic activity as revealed by *in vitro* cell culture studies with primary lung fibroblasts and *in vivo* studies using a BLM-induced pulmonary fibrosis model mouse. SCGB3A2, a member of the SCGB gene superfamily composed of secretory proteins of small molecular weight, is predominantly expressed in lung airways (14, 43). The most studied member of the SCGB gene superfamily, namely SCGB1A1, also called uteroglobin, Clara cell 10-kDa protein, or Clara cell secretory protein, is a multifunctional protein with anti-inflammatory/immunomodulatory properties with manifestation of antichemotactic, antiallergic, antitumorigenic, and embryonic growth-stimulatory activities (19). The current study revealed that the related pro-

TABLE 1
GO terms for overexpressed genes in BLM-injured lung

Gene ontology term	Cluster frequency[a]	Total frequency[b]	Corrected p value[c]
	%	%	
Biological Process, cell adhesion	6.40	3.50	2.92×10^{-5}
Biological adhesion	6.40	3.50	2.92×10^{-5}
Antigen processing and presentation of exogenous peptide antigen	0.70	0.10	0.00654
Immune system process	6.30	3.90	0.01711
Inflammatory response	2.70	1.30	0.01977
Antigen processing and presentation of peptide antigen via MHC class II	0.60	0.10	0.02221
Antigen processing and presentation of exogenous peptide antigen via MHC class II	0.60	0.10	0.02221
Antigen processing and presentation of peptide of polysaccharide antigen via MHC class II	0.60	0.10	0.04108
Response to wounding	3.30	1.80	0.04663
Cellular Component			
Extracellular region part	18.00	12.70	5.62×10^{-7}
Extracellular matrix	4.00	1.70	1.05×10^{-6}
Proteinaceous extracellular matrix	3.39	1.70	1.68×10^{-6}
Extracellular region	20.40	15.10	5.57×10^{-6}
Extracellular space	16.80	12.00	7.62×10^{-6}
Molecular function			
Carbohydrate binding	3.00	1.60	0.04087

[a] Frequency of Entrez Gene IDs appeared in a given GO term based on those having over 0.585 in log ratio.
[b] Frequency of Entrez Gene IDs appeared in a given GO term based on all genes.
[c] p value corrected using the Bonferroni method.

TABLE 2
GO terms for suppressed genes by SCGB3A2 in BLM-injured lung

Gene ontology term	Cluster frequency[a]	Total frequency[b]	Corrected p value[c]
	%	%	
Biological process			
Defense response	6.10	2.50	6.78×10^{-5}
Response to external stimulus	6.40	2.70	7.91×10^{-5}
Response to wounding	4.50	1.80	0.00172
Response to stimulus	15.80	10.60	0.00896
Inflammatory response	3.20	1.30	0.03692
Cellular component			
Extracellular region	24.50	15.10	1.82×10^{-9}
Extracellular region part	20.40	12.70	2.26×10^{-7}
Extracellular space	19.50	12.00	3.22×10^{-7}

[a] Frequency of Entrez Gene IDs appeared in a given GO term based on those having over 0.585 in log ratio.
[b] Frequency of Entrez Gene IDs appeared in a given GO term based on all genes.
[c] p value corrected using the Bonferroni method.

TABLE 3
GO terms overexpressed by SCGB3A2 in normal lung

Gene ontology term, molecular function	Cluster frequency[a]	Total frequency[b]	Corrected p value[c]
	%	%	
Signal transducer activity	20.7	15.9	0.0378
Molecular transducer activity	20.7	15.9	0.0378

[a] Frequency of Entrez Gene IDs appeared in a given GO term based on those having over 0.585 in log ratio.
[b] Frequency of Entrez Gene IDs appeared in a given GO term based on all genes.
[c] p value corrected using the Bonferroni method.

tein SCGB3A2 at therapeutic levels has novel biological activity toward induced fibrosis in addition to its known anti-inflammatory (24) and growth factor activities (25). SCGB1A1 was previously suggested to be a novel cytokine (44). The current results support the notion that the SCGB gene superfamily may be a novel cytokine family. The anti-inflammatory, growth factor and anti-fibrotic activities that SCGB3A2 possesses may suggest a potential use for this protein in the treatment of many lung diseases, including lung fibrosis as demonstrated in this study.

BLM administered by intratracheal intubation induced pulmonary fibrosis, which focally occupied the pulmonary parenchyma by 3 weeks after BLM administration. Interestingly, BLM-induced fibrosis was almost completely suppressed by SCGB3A2 treatment, which interfered with the infiltration of neutrophils and macrophages into lung and the expression of fibrosis related-genes such as collagens, fibronectin, elastin, cathepsins, and MMPs, all of which were up-regulated by BLM. The development of fibrosis was hardly detectable by the end of 2 weeks after BLM administration, suggesting that SCGB3A2 might inhibit development of fibrosis when given at its early stages.

The anti-fibrotic activity of SCGB3A2 appears to be exerted through STAT1 phosphorylation, induction of SMAD7, and inhibition of SMAD2/3 phosphorylation, which results in suppression of the TGFβ signaling, ultimately leading to the inhibition of myofibroblasts formation. Interestingly, this is the exact pathway that IFNγ exhibits its anti-fibrotic activity (9, 35). We initially hypothesized that SCGB3A2 may induce the expression of IFNγ, thereby suppressing TGFβ signaling. However, the SCGB3A2 pathway is likely to be distinct from the IFNγ pathway based on the following reasons; 1) IFNγ-induced phosphorylation of STAT1 and increased expression of SMAD7 usually occurs within 10–30 min after IFNγ stimulation (supplemental Fig. S3) (9, 41, 42, 45), whereas it took ~3 h for SCGB3A2 to induce maximum levels of STAT1 phosphorylation, 2) SCGB3A2 did not induce IFNγ mRNA expression as determined by RT-PCR, 3) IFNγ receptor neutralizing antibody (46) did not block SCGB3A2-induced STAT1 phosphorylation, and 4) CHX ablated the expression of pSTAT1 in fibroblasts treated with SCGB3A2 but not IFNγ. These results suggest the involvement of a newly synthesized protein upon SCGB3A2 stimulation other than IFNγ in the SCGB3A2-pSTAT1 pathway. In this regard it is interesting to note that STAT1 was induced by SCGB3A2 in a CHX-sensitive fashion. SMAD7 was also induced by SCGB3A2. The SCGB3A2-induced increase of STAT1 and SMAD7 expression was dramatically inhibited by TGFβ at the mRNA levels. However the pSTAT1/STAT1 ratio stayed the same. The involvement of STAT1 in the SCGB3A2 pathway was confirmed by STAT1 siRNA experiments, in which no decrease of αSMA was observed in

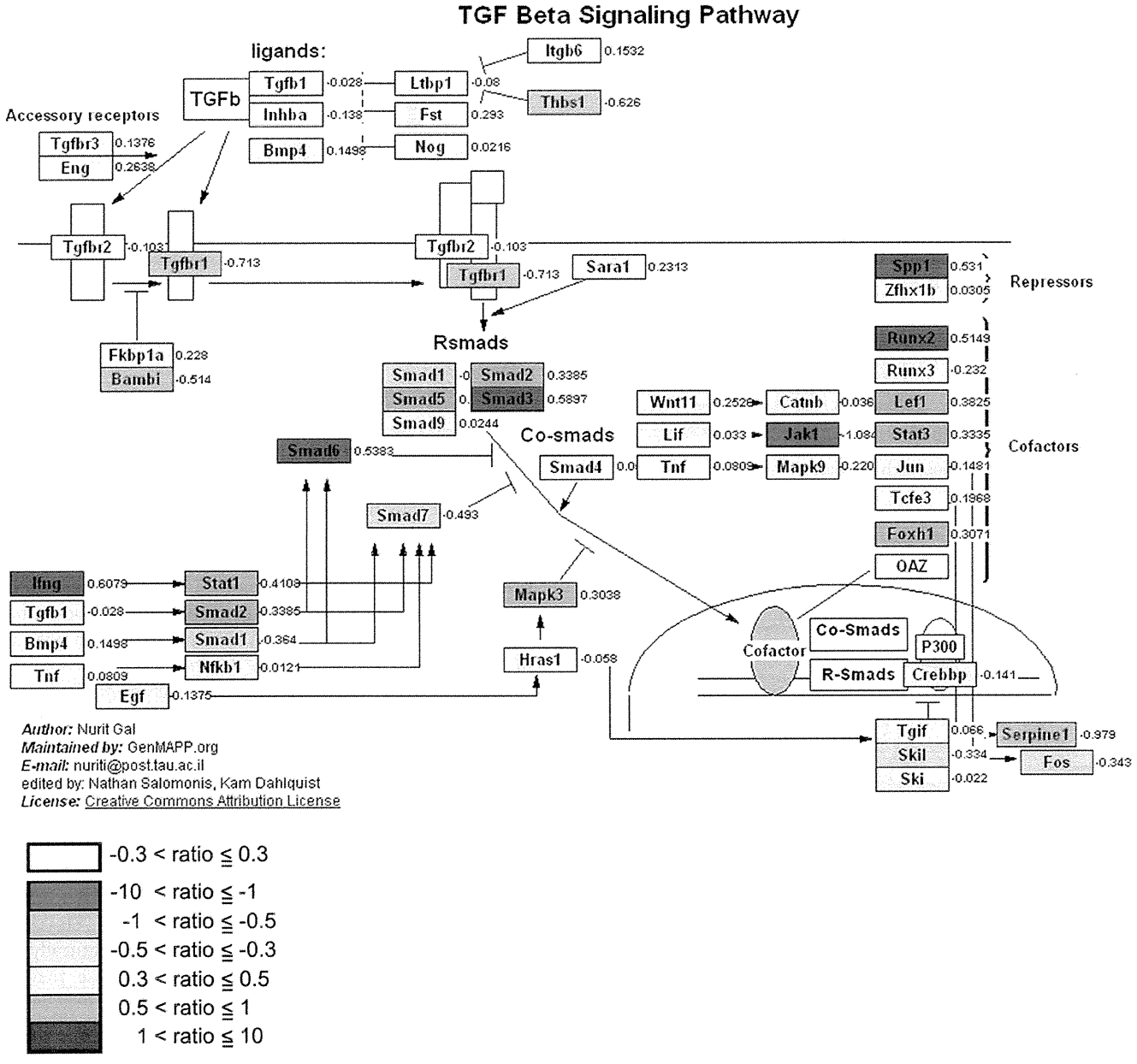

FIGURE 5. **Effect of SCGB3A2 on TGFβ signaling pathway.** Pathway analysis of microarray data showed that the TGFβ signaling pathway was affected by administration of SCGB3A2. Median -fold differences from seven separate samples for each gene on which microarray analysis were run are color-coded based on the *scale* shown at the *bottom left*.

TGFβ+SCGB3A2-treated cells as compared with TGFβ only treatment. These results together suggest that the SCGB3A2-pSTAT1-SMAD7 signaling pathway may be through a SCGB3A2-specific receptor that is distinct from the IFNγ receptor (Fig. 7). We previously suggested the presence of a SCGB3A2-specific receptor-like molecule on the surface of pulmonary mesenchymal cells (25). The nature of the CHX-sensitive intermediate molecule(s), a SCGB3A2-specific receptor, and the mechanism(s) for the inhibitory effect of TGFβ on the induction of STAT1 and SMAD7 by SCGB3A2 are currently not known. Further experiments are required to address these questions. Other cytokines/molecules such as IFNα, IFNβ, epidermal growth factor, growth hormone, and estrogen are known to activate STAT1 (47). Among them, neither IFNα nor IFNβ was induced by SCGB3A2 in mouse lung primary fibroblasts, suggesting that they are not likely involved in the SCGB3A2-pSTAT1-SMAD7 pathway. The involvement of the other cytokines/molecules in the SCGB3A2-pSTAT1 pathway needs to be examined.

Inflammation is the first to occur after BLM administration followed by fibrosis (3–6). In animal models the fibrosis stage starts ~1 week after BLM administration (3). In our BLM model, SCGB3A2 was administered at the fibrosis period and exhibited anti-fibrotic activity through blocking the TGFβ signaling pathway. We previously demonstrated using mice-exogenously administered SCGB3A2 that SCGB3A2

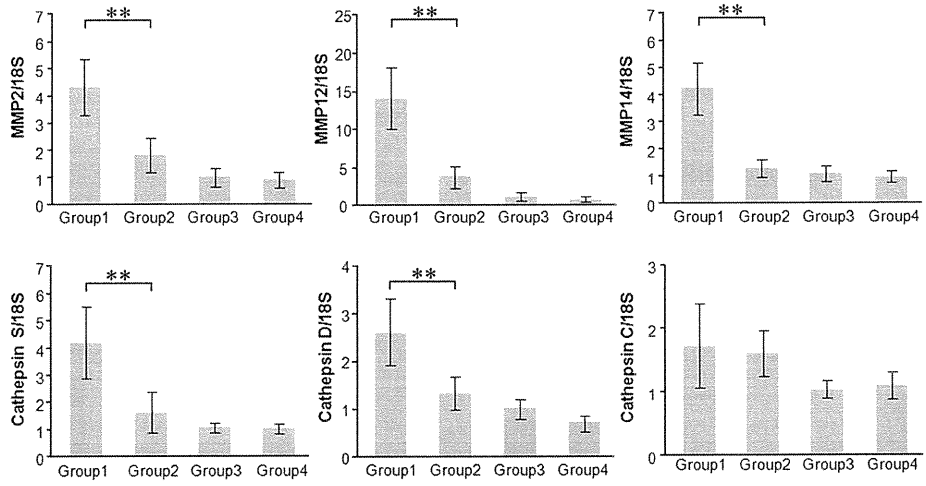

FIGURE 6. **Confirmation of microarray data by qRT-PCR.** Expression levels of MMP2, MMP12, MMP14, cathepsin S, cathepsin D, and cathepsin C mRNAs relative to 18 S were determined by qRT-PCR using mRNAs prepared from mouse lungs of Groups 1–4 as described in Fig. 4. The *graph* shows the mean ± S.D. from 4–9 lungs per group, each in triplicate. **, $p < 0.01$.

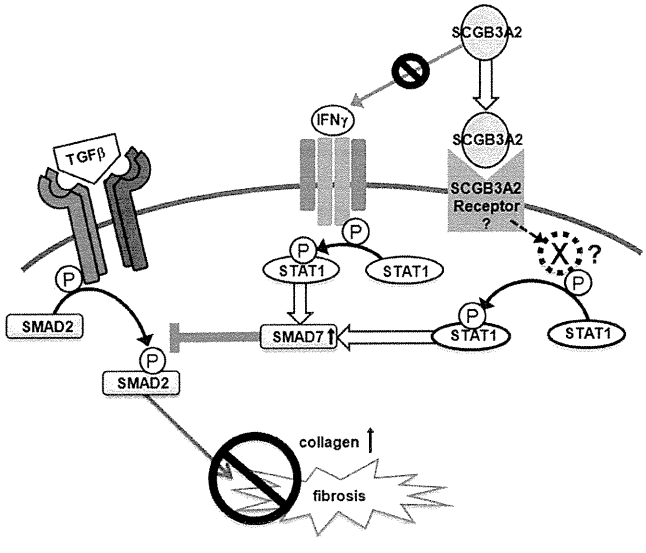

FIGURE 7. **Schematic diagram for the SCGB3A2-induced inhibition of the TGFβ signaling pathway.** SCGB3A2 inhibits collagen production through STAT1 phosphorylation and increases expression of SMAD7, which inhibits TGFβ-mediated SMAD2/3 activation. A newly synthesized molecule *X* mediates the SCGB3A2-induced STAT1 phosphorylation.

exhibits anti-inflammatory activities. We do not know whether SCGB3A2, if administered at the beginning of BLM administration, exerts anti-inflammatory activities and reduces the damage otherwise caused by BLM. Furthermore, we do not know whether endogenous SCGB3A2 regulates pulmonary inflammation and/or fibrosis. However, the following evidence suggests a role for SCGB3A2 in inflammation in lung *in vivo*; in the ovalbumin-induced allergic airway inflammation model mouse, SCGB3A2 expression is reduced in the airways (24, 48, 49), and the plasma SCGB3A2 levels are significantly lower in severe asthmatics without oral corticosteroid treatment as compared with mild- or moderate-asthma patients and controls (50). In the current study, a rather strong focal SCGB3A2 expression was found in a part of epithelial cells, and overexpressed SCGB3A2 was accumulated in fibrotic foci of lungs of mice subjected to BLM. However, it should be noted that these lungs are already at late stages, having developed BLM-induced fibrosis. In BLM+SCGB3A2-treated lungs, SCGB3A2 expression is in similar patterns but is slightly up-regulated to those found in control mice. Whether SCGB3A2 is down-regulated right after BLM administration needs to be determined.

Although IFNγ has been used as a therapy for pulmonary fibrosis (5, 6, 12), it causes a number of potentially harmful side effects and thus is not useful for advanced fibrosis (nlm.nih.gov (13)). In this study SCGB3A2 signaling was found to cross-talk with the IFNγ except at the beginning of the pathway. This suggests that SCGB3A2 could be potentially useful in treating fibrosis, in particular pulmonary fibrosis. More importantly, SCGB3A2 can be administered intratracheally. SCGB3A2 is almost exclusively expressed in lung (14) and is present at relatively high levels in the BALF of normal lungs (24). Thus, delivering a protein into a place where the protein is naturally present in high amounts would probably not cause toxicities. Alternatively, SCGB3A2 can be administered intravenously. Indeed, SCGB3A2 growth factor activity was previously demonstrated *in vivo* by intravenous administration of SCGB3A2 to pregnant female mice through the tail vein resulting in advanced development of fetal lungs (25). In that study, no gross abnormalities were observed in any fetal organs after intravenous SCGB3A2 administration. Furthermore, histological examination of the dam's lung did not show any abnormalities. Based on these facts, it is likely that SCGB3A2 may potentially improve pulmonary fibrosis without harmful side effects as seen with IFNγ. It is possible that BLM treatment as a chemotherapy reagent may not damage the lung if SCGB3A2 is given at the same time. However, additional studies are necessary to determine the efficacy of SCGB3A2 in treating pulmonary fibrosis in humans.

In conclusion, the present study demonstrated that SCGB3A2 inhibits TGFβ signaling through increased STAT1 phosphorylation and expression of SMAD7 and decreased phosphorylation of SMAD2/3, leading to inhibition of myofi-

broblast differentiation. The inhibitory effect of SCGB3A2 on myofibroblast differentiation was reproduced using a BLM-induced lung fibrosis model mouse, in which the severity of lung fibrosis was reduced by SCGB3A2 administration.

Acknowledgments—We thank Drs. Lalage Wakefield, Kathleen Flanders, and Frank Gonzalez (NCI, National Institutes of Health) for advice and critical review of the manuscript and Michie Kobayashi for microarray analysis (DNA Chip Research Inc., Yokohama, Japan).

REFERENCES

1. Coultas, D. B., Zumwalt, R. E., Black, W. C., and Sobonya, R. E. (1994) *Am. J. Resp. Crit. Care Med.* **150,** 967–972
2. Crystal, R. G., Bitterman, P. B., Mossman, B., Schwarz, M. I., Sheppard, D., Almasy, L., Chapman, H. A., Friedman, S. L., King, T. E., Jr., Leinwand, L. A., Liotta, L., Martin, G. R., Schwartz, D. A., Schultz, G. S., Wagner, C. R., and Musson, R. A. (2002) *Am. J. Respir. Crit. Care Med.* **166,** 236–246
3. Moeller, A., Ask, K., Warburton, D., Gauldie, J., and Kolb, M. (2008) *Int. J. Biochem. Cell Biol.* **40,** 362–382
4. Cutroneo, K. R., White, S. L., Phan, S. H., and Ehrlich, H. P. (2007) *J. Cell. Physiol.* **211,** 585–589
5. Tzortzaki, E. G., Antoniou, K. M., Zervou, M. I., Lambiri, I., Koutsopoulos, A., Tzanakis, N., Plataki, M., Maltezakis, G., Bouros, D., and Siafakas, N. M. (2007) *Respir. Med.* **101,** 1821–1829
6. Wynn, T. A. (2004) *Nat. Rev. Immunol.* **4,** 583–594
7. Eickelberg, O., Pansky, A., Koehler, E., Bihl, M., Tamm, M., Hildebrand, P., Perruchoud, A. P., Kashgarian, M., and Roth, M. (2001) *FASEB J.* **15,** 797–806
8. Ghosh, A. K., and Varga, J. (2007) *J. Cell. Physiol.* **213,** 663–671
9. Ulloa, L., Doody, J., and Massagué, J. (1999) *Nature* **397,** 710–713
10. Zhang, S., Fei, T., Zhang, L., Zhang, R., Chen, F., Ning, Y., Han, Y., Feng, X. H., Meng, A., and Chen, Y. G. (2007) *Mol. Cell Biol.* **27,** 4488–4499
11. Scotton, C. J., and Chambers, R. C. (2007) *Chest* **132,** 1311–1321
12. Puente, N. A., Aliotta, J. M., and Passero, M. A. (2007) *Med. Health R. I.* **90,** 43–45
13. Selman, M. (2003) *Am. J. Respir. Crit. Care Med.* **167,** 945–946
14. Niimi, T., Keck-Waggoner, C. L., Popescu, N. C., Zhou, Y., Levitt, R. C., and Kimura, S. (2001) *Mol. Endocrinol.* **15,** 2021–2036
15. Reynolds, S. D., Reynolds, P. R., Pryhuber, G. S., Finder, J. D., and Stripp, B. R. (2002) *Am. J. Respir. Crit. Care Med.* **166,** 1498–1509
16. Klug, J., Beier, H. M., Bernard, A., Chilton, B. S., Fleming, T. P., Lehrer, R. I., Miele, L., Pattabiraman, N., and Singh, G. (2000) *Ann. N.Y. Acad. Sci.* **923,** 348–354
17. Shijubo, N., Kawabata, I., Sato, N., and Itoh, Y. (2003) *Curr. Pharm. Des.* **9,** 1139–1149
18. Wang, S. Z., Rosenberger, C. L., Bao, Y. X., Stark, J. M., and Harrod, K. S. (2003) *J. Immunol.* **171,** 1051–1060
19. Mukherjee, A. B., Zhang, Z., and Chilton, B. S. (2007) *Endocr. Rev.* **28,** 707–725
20. Mandal, A. K., Zhang, Z., Ray, R., Choi, M. S., Chowdhury, B., Pattabiraman, N., and Mukherjee, A. B. (2004) *J. Exp. Med.* **199,** 1317–1330
21. Miele, L. (2000) *Ann. N.Y. Acad. Sci.* **923,** 128–140
22. Watson, M. A., and Fleming, T. P. (1996) *Cancer Res.* **56,** 860–865
23. Culleton, J., O'Brien, N., Ryan, B. M., Hill, A. D., McDermott, E., O'Higgins, N., and Duffy, M. J. (2007) *Int. J. Cancer* **120,** 1087–1092
24. Chiba, Y., Kurotani, R., Kusakabe, T., Miura, T., Link, B. W., Misawa, M., and Kimura, S. (2006) *Am. J. Respir. Crit. Care Med.* **173,** 958–964
25. Kurotani, R., Tomita, T., Yang, Q., Carlson, B. A., Chen, C., and Kimura, S. (2008) *Am. J. Respir. Crit. Care Med.* **178,** 389–398
26. Bin, L. H., Nielson, L. D., Liu, X., Mason, R. J., and Shu, H. B. (2003) *J. Immunol.* **171,** 924–930
27. Maeng, H. G., Lim, H., Jeong, Y. J., Woo, A., Kang, J. S., Lee, W. J., and Hwang, Y. I. (2009) *Immunobiology* **214,** 311–320
28. Lin, Y. C., Huang, D. Y., Chu, C. L., and Lin, W. W. (2010) *Mol. Immunol.* **47,** 1569–1578
29. Asazuma-Nakamura, Y., Dai, P., Harada, Y., Jiang, Y., Hamaoka, K., and Takamatsu, T. (2009) *Exp. Cell Res.* **315,** 1190–1199
30. Kurotani, R., Yoshimura, S., Iwasaki, Y., Inoue, K., Teramoto, A., and Osamura, R. Y. (2002) *J. Endocrinol.* **172,** 477–487
31. Ashburner, M., Ball, C. A., Blake, J. A., Botstein, D., Butler, H., Cherry, J. M., Davis, A. P., Dolinski, K., Dwight, S. S., Eppig, J. T., Harris, M. A., Hill, D. P., Issel-Tarver, L., Kasarskis, A., Lewis, S., Matese, J. C., Richardson, J. E., Ringwald, M., Rubin, G. M., and Sherlock, G. (2000) *Nat. Genet.* **25,** 25–29
32. Doniger, S. W., Salomonis, N., Dahlquist, K. D., Vranizan, K., Lawlor, S. C., and Conklin, B. R. (2003) *Genome Biol.* **4,** R7
33. Tomasek, J. J., Gabbiani, G., Hinz, B., Chaponnier, C., and Brown, R. A. (2002) *Nat. Rev. Mol. Cell Biol.* **3,** 349–363
34. Shoulders, M. D., and Raines, R. T. (2009) *Annu. Rev. Biochem.* **78,** 929–958
35. Weng, H., Mertens, P. R., Gressner, A. M., and Dooley, S. (2007) *J. Hepatol.* **46,** 295–303
36. Yu, H., Pardoll, D., and Jove, R. (2009) *Nat. Rev. Cancer* **9,** 798–809
37. Luppi, F., Losi, M., D'Amico, R., Fabbri, L. M., and Richeldi, L. (2009) *Sarcoidosis Vasc. Diffuse Lung Dis.* **26,** 64–68
38. Azuma, A., Li, Y. J., Abe, S., Usuki, J., Matsuda, K., Henmi, S., Miyauchi, Y., Ueda, K., Izawa, A., Sone, S., Hashimoto, S., and Kudoh, S. (2005) *Am. J. Respir. Cell Mol. Biol.* **32,** 93–98
39. Senft, A. P., Taylor, R. H., Lei, W., Campbell, S. A., Tipper, J. L., Martinez, M. J., Witt, T. L., Clay, C. C., and Harrod, K. S. (2010) *Am. J. Respir. Cell Mol. Biol.* **42,** 404–414
40. Papatheodoridis, G. V., Petraki, K., Cholongitas, E., Kanta, E., Ketikoglou, I., and Manesis, E. K. (2005) *J. Viral. Hepat.* **12,** 199–206
41. Tamai, M., Kawakami, A., Tanaka, F., Miyashita, T., Nakamura, H., Iwanaga, N., Izumi, Y., Arima, K., Aratake, K., Huang, M., Kamachi, M., Ida, H., Origuchi, T., and Eguchi, K. (2006) *J. Lab. Clin. Med.* **147,** 182–190
42. Seo, J. Y., Kim, D. Y., Lee, Y. S., and Ro, J. Y. (2009) *Cytokine* **46,** 51–60
43. Tomita, T., Kido, T., Kurotani, R., Iemura, S., Sterneck, E., Natsume, T., Vinson, C., and Kimura, S. (2008) *J. Biol. Chem.* **283,** 25617–25627
44. Mukherjee, A. B., Kundu, G. C., Mantile-Selvaggi, G., Yuan, C. J., Mandal, A. K., Chattopadhyay, S., Zheng, F., Pattabiraman, N., and Zhang, Z. (1999) *Cell. Mol. Life Sci.* **55,** 771–787
45. Lee, Y. J., and Benveniste, E. N. (1996) *J. Immunol.* **157,** 1559–1568
46. Cheng, M., Nguyen, M. H., Fantuzzi, G., and Koh, T. J. (2008) *Am. J. Physiol. Cell Physiol.* **294,** C1183–C1191
47. Krämer, O. H., and Heinzel, T. (2010) *Mol. Cell Endocrinol.* **315,** 40–48
48. Chiba, Y., Kusakabe, T., and Kimura, S. (2004) *Am. J. Physiol. Lung Cell Mol. Physiol.* **287,** L1193–L1198
49. Chiba, Y., Srisodsai, A., Supavilai, P., and Kimura, S. (2005) *Immunol. Lett.* **97,** 123–129
50. Inoue, K., Wang, X., Saito, J., Tanino, Y., Ishida, T., Iwaki, D., Fujita, T., Kimura, S., and Munakata, M. (2008) *Allergol. Int.* **57,** 57–64

J Physiol Sci (2011) 61:167–179
DOI 10.1007/s12576-011-0133-3

ORIGINAL PAPER

DNA microarray profiling identified a new role of growth hormone in vascular remodeling of rat ductus arteriosus

Mei-Hua Jin · Utako Yokoyama · Yoji Sato · Aki Shioda · Qibin Jiao · Yoshihiro Ishikawa · Susumu Minamisawa

Received: 3 December 2010 / Accepted: 28 December 2010 / Published online: 2 February 2011

Abstract The ductus arteriosus (DA), a fetal arterial connection between the pulmonary artery and the aorta, has a character distinct from the adjacent arteries. We compared the transcriptional profiles of the DA and the aorta of Wistar rat fetuses on embryonic day 19 (preterm) and day 21 (near-term) using DNA microarray analyses. We found that 39 genes were expressed 2.5-fold greater in the DA than in the aorta. Growth hormone (GH) receptor (GHR) exhibited the most significant difference in expression. Then, we found that GH significantly promoted migration of DA smooth muscle cells (SMCs), thus enhancing the intimal cushion formation of the DA explants. GH also regulated the expression of cytoskeletal genes in DA SMCs, which may retain a synthetic phenotype in the smooth muscle-specific cytoskeletal genes. Thus, the present study revealed that GH-GHR signal played a role in the vascular remodeling of the DA.

Keywords Growth hormone · Gene expression · Vascular remodeling · Premature infant · Congenital heart disease

Electronic supplementary material The online version of this article (doi:10.1007/s12576-011-0133-3) contains supplementary material, which is available to authorized users.

M.-H. Jin · U. Yokoyama · A. Shioda · Y. Ishikawa (✉) · S. Minamisawa (✉)
Cardiovascular Research Institute, Yokohama City University, 3-9 Fukuura, Kanazawa-ku, Yokohama 236-0004, Japan
e-mail: yishikaw@med.yokohama-cu.ac.jp

S. Minamisawa
e-mail: sminamis@waseda.jp

Y. Sato
Division of Cellular and Gene Therapy Products, National Institute of Health Sciences, 1-18-1 Kamiyoga, Setagaya-ku, Tokyo 158-8501, Japan

Q. Jiao · S. Minamisawa
Department of Life Science and Medical Bioscience, Waseda University Graduate School of Advanced Science and Engineering, 2-2 Wakamatsucho, Shinjuku-ku, Tokyo 162-8480, Japan

Introduction

The ductus arteriosus (DA), a fetal arterial connection between the pulmonary artery and the descending aorta, is essential to fetal life. The morphology and function of the DA dramatically change during development [1]. In particular, during late gestation, the deposition of extracellular matrix in the subendothelium is increased, and the smooth muscle cells (SMCs) of the media migrate into this region, resulting in intimal thickening [2]. This vascular remodeling of the DA is essential for its postnatal closure and is not observed in adjacent arteries. Thus, the DA has distinct characteristic features that differ from those of the adjacent arteries (the aorta and pulmonary arteries). This characteristic of the DA is largely dependent on the expression of the distinct subsets of genes involved in the developmental vascular remodeling that occurs during gestation. To understand the precise transcriptional network in the DA, genome-wide analysis is a powerful approach that can be utilized. In this context, several studies, including ours, have been carried out to identify the effects of oxygen [3] or maternal administration of vitamin A [4] on the transcriptional profiles of the DA. Although the study by Costa et al. [3] is the only one that demonstrated the characteristic differences in the transcriptional profiles between rat DA and the aorta of premature fetuses and neonates, they analyzed their transcriptional profiles on embryonic day 19 (e19) only; they did not examine the changes during later gestation.

Because the morphological and physiological characteristics of the DA differ significantly between premature and mature fetuses [1], it is of great interest to investigate the transcriptional profiles of the DA and the adjacent aorta in the remodeling process that occurs during late gestation.

Materials and methods

Tissue collection for DNA microarray and quantitative reverse transcription polymerase chain reaction analyses

Pooled tissues from the DA or the aorta were obtained from Wistar rat embryos on e19 ($n \geq 120$) and e21 ($n \geq 120$). Reverse transcription polymerase chain reaction (RT-PCR) analysis was performed as described previously [2]. The information on PCR primers for RT-PCR analyses is provided in Supplemental data 1.

Total RNA preparation and DNA microarray analysis

Total RNA preparation and DNA microarray analysis were performed as described previously [4]. Briefly, total RNA was converted to biotin-labeled cRNA that was hybridized to rat genome U34A GeneChip DNA microarray (Affymetrix, Santa Clara, CA). The hybridization experiments were performed in duplicate and the intensities were averaged. If the difference in the signal intensities of a given sequence tag was equal to the cutoff (=2.5-fold) or more, and if the "Comparison Analysis" of the Microarray Suite Software indicated "increased" or "decreased" with the ≥2.5-fold difference at any developmental stage, that sequence tag was considered to exhibit a significant difference between the DA and the aorta.

Primary culture of rat DA SMCs

Vascular SMCs in primary culture were obtained from the DAs of Wistar rat embryos at e21. The tissues were minced and transferred to a 1.5-ml centrifuge tube that contained 800 μl of collagenase-dispase enzyme mixture [1.5 mg/ml collagenase-dispase (Roche), 0.5 mg/ml elastase type II-A (Sigma Immunochemicals, St. Louis, MO), 1 mg/ml trypsin inhibitor type I-S (Sigma), and 2 mg/ml bovine serum albumin fraction V (Sigma) in Hanks' balanced salt solution (Sigma)]. The digestion was carried out at 37°C for 15–20 min. Then cell suspensions were centrifuged, and the medium was changed to the collagenase II enzyme mixture [1 mg/ml collagenase II (Worthington), 0.3 mg/ml trypsin inhibitor type I–S, and 2 mg/ml bovine serum albumin fraction V in Hanks' balanced salt solution]. After 12 min of incubation at 37°C, cell suspensions were transferred to growth medium in 35-mm poly-L-lysine (Sigma)-coated dishes in a moist tissue culture incubator at 37°C in 5% CO_2, 95% ambient mixed air. The growth medium contained Dulbecco's modified Eagle's medium (DMEM) with 10% fetal bovine serum (FBS) and 1% penicillin-streptomycin solution (Sigma). The confluent cells were used at passages 4–6.

SMC migration assay

The migration assay was performed using 24-well Transwell culture inserts with polycarbonate membranes (8-μm pores; Corning Inc.) coated with fibronectin. The DA SMCs were harvested with trypsin-ethylenediamine tetraacetic acid (EDTA), resuspended in serum-free DMEM, and distributed at a density of 1×10^5 cells/100 μl in the inserts. The cells were allowed to settle in serum-free DMEM for 1 h before the addition of GH (20 and 200 ng/ml) in the lower chamber. Under basal conditions, the lower chambers were filled with 600 μl serum-free DMEM. SMCs were then allowed to migrate to the underside of the insert's membrane at 37°C/5% CO_2. At the end of the experiment, the cells were fixed in 10% buffered formalin. SMCs were stained with Cyto Quick (Muto Pure Chemicals), and cells on the upper surface of the membrane were mechanically removed with a cotton swab. Cells that migrated onto the lower surface of the membrane were manually counted from three different fields (0.5 mm^2/field) under a microscope.

Cell proliferation assays

[^{3}H]thymidine incorporation was used to measure cell proliferation in DA SMCs. The SMCs were reseeded into a 24-well culture plate at an initial density of 1×10^5 cells per well for 24 h before serum starvation with DMEM containing 0.1% FBS. Cells were then incubated with or without GH (20 and 200 ng/ml) for 24 h in the starvation medium before addition of 1 μCi of [*methyl*-^{3}H]thymidine (specific activity 5 Ci/mM; Amersham International, Bucks, UK) for 4 h at 37°C. After fixation with 1.0 ml of 10% trichloroacetic acid, the cells were solubilized with 0.5 ml of 0.5 M NaOH and then neutralized with 0.25 ml of 1 N HCl. A liquid scintillation counter was used to measure [^{3}H]thymidine incorporation. Data obtained from triplicate wells were averaged.

Quantitation of hyaluronan

The amount of hyaluronan in the cell culture supernatant was measured by a latex agglutination method based on the specific interaction of hyaluronan with the latex-labeled hyaluronan-binding protein from bovine cartilage (Fujirebio Inc.). Hyaluronan was quantified in duplicate according to

the manufacturer's instructions using 2.5-μl aliquots of the conditioned cell culture medium using the HITACHI 7070 analysis system (Hitachi) at an 800-nm wavelength.

Organ culture

Fetal arteries including the DA and the aortic arch arteries were incubated with GH (200 ng/ml) for 72 h in serum-free DMEM as described previously [2]. Explants were then fixed in 10% buffered formalin and embedded in paraffin. The sectioned segments in the middle portion of the DA were analyzed histochemically.

Immunohistochemistry

Tissue staining and immunohistochemistry were performed as described previously [5, 6]. Mouse monoclonal anti-GHR antibody (MAB263) was purchased from Abcam (Tokyo, Japan).

Statistics

Data are presented as mean ± standard error (SEM) of independent experiments. Statistical analysis was performed between two groups by unpaired two-tailed Student's *t* test or unpaired *t* test with Welch correction, and among multiple groups by one-way analysis of variance (ANOVA) followed by Neuman-Keuls multiple comparison test. A p value of <0.05 was considered significant.

Results

Genes differentially expressed between the DA and the aorta

All the microarray data in the present study were deposited at the Gene Expression Omnibus (GEO) repository (http://www.ncbi.nlm.nih.gov/projects/geo/; accession no. GSE3422). A total of 117 genes (142 probe sets) showed a significant difference (≥2.5-fold) between the DA and the aorta at e19 or e21. Among 117 genes, 39 (43 probe sets) exhibited a DA-dominant expression pattern (Table 1), and 78 (99 probe sets) exhibited an aorta-dominant expression pattern (Table 2).

Of 39 genes in the DA-dominant expression pattern (Table 1), 34 had a known function, and 3 were homologous to known genes. Although several genes, such as prostaglandin E receptor 4 (subtype EP4) (Ptger4) and endothelin-1, are known to play an important role in the regulation of vascular tone of the DA [1], the role of most of the other genes in the DA has not been identified. We found that growth hormone (GH) receptor exhibited the highest difference in the expression between the DA and the aorta among 39 DA-dominant genes.

Of the 39 genes, 9 encode proteins related to cytoskeleton and the extracellular matrix, including sarcomeric genes such as Myh11 (myosin heavy chain 11), Myl6 (myosin light chain, polypeptide 6, alkali, smooth muscle and non-muscle), Actg2 (actin, gamma 2), Tpm1 (tropomyosin 1, alpha), Tnn (tenascin N, predicted), and Lamb2 (laminin beta2). Three membrane ion channels, ATPase Na^+/K^+ transporting b1 polypeptide and potassium inwardly rectifying channel (Atp1b1), subfamily J, member 8 (Kcnj8), which is known as ATP-sensitive potassium channel K_{ATP}-1, and Ca^{2+} channel, voltage-dependent, $\alpha 2/\delta$ subunit 1 (Cacna2d1), were also strongly expressed in the DA.

We also identified 79 genes in the aorta-dominant expression pattern (Table 2). Of the 79 genes, 14 genes encode proteins related to cytoskeleton and the extracellular matrix. Cardiac sarcomeric genes such as Myh6 (myosin heavy chain, polypeptide 6), Myh7 (myosin heavy chain, polypeptide 7), Myl7 (myosin, light polypeptide 7, regulatory), Myl2 (myosin regulatory light chain 2, ventricular/cardiac muscle isoform), Actc1 (alpha, actin alpha cardiac 1), Tnnt2 (troponin T2, cardiac), Tnni3 (troponin I, cardiac), and Fn1 (fibronectin 1) were more highly expressed in the aorta than in the DA. Accordingly, there was a marked difference in the composition of the genes related to the cytoskeleton and the extracellular matrix between the DA and the aorta. Sixteen genes were expressed 2.5-fold more in the aorta at both e19 and e21 than in the DA, whereas 24 genes were expressed 2.5-fold more in the aorta than in the DA only at e21. To confirm the results of the DNA microarray, we performed RT-PCR (Supplemental data 2).

Growth hormone receptor mRNA and protein were dominantly expressed in the developing DA

As mentioned above, GH receptor (GHR) exhibited the highest difference of expression between the DA and the aorta (Fig. 1a), suggesting that GH-GHR signal plays a distinct role in the vascular remodeling of the DA from the aorta. The expression of GH mRNA was very low, and there was no difference between the DA and the aorta (Fig. 1b). Interestingly, the expression levels of insulin-like growth factor (IGF)-I and IGF-II mRNAs were higher in the aorta than in the DA, whereas the expression levels of IGF-I receptor (IGF-IR) and IGF-IIR mRNAs did not differ (Fig. 1c–f). In addition, the expression levels of IGF binding protein (IGFBP) 2 and IGFBP5 mRNAs were also higher in the aorta than in the DA at e21 and at e19, respectively (Table 2).

The expression of GHR mRNA was also confirmed by quantitative RT-PCR analyses. We found that the expression levels of GHR mRNA were higher in the rat DA than

Table 1 DA-dominant genes

	Probe set ID	RefSeq Transcript ID	Gene title	Gene symbol	Fold difference between DA and aorta	
					e19	e21
1	**rc_AI104225_at**	**NM_017094**	**Growth hormone receptor**	**Ghr**	**5.0**	**8.7**
2	Z83757mRNA_at	XM_222794	Tenascin N (predicted)	Tnn_predicted	2.3	7.4
3	L16764_s_at/// Z75029_s_at	NM_031971/// NM_212504	Heat shock 70kD protein 1A///heat shock 70kD protein 1B	Hspa1a///Hspa1b	8.6	7.1
4	rc_AA891527_at	NM_022531	Desmin	Des	1.4	6.3
5	rc_AA893846_at	NM_053591	Dipeptidase 1 (renal)	Dpep1	3.4	5.6
6	X73524_at	NM_013129	Interleukin 15	Il15	2.0	5.6
7	D28561_s_at	NM_031677	Four and a half LIM domains 2	Fhl2	3.4	4.9
8	rc_AA894200_at	XM_342032	Proprotein convertase subtilisin/kexin type 5	Pcsk5	1.4	4.8
9	AF002281_at	NM_012870	Tumor necrosis factor receptor superfamily, member 11b (osteoprotegerin)	Tnfrsf11b	1.2	4.7
10	M22323_at	NM_013086/// NM_017334	cAMP responsive element modulator	Crem	1.8	3.5
11	U94330_at	NM_001007678	Mss4 protein	Mss4	1.5	3.1
12	rc_AA799773_at	NM_134410	Mg87 protein	Mg87	1.3	2.9
13	X82152_at	NM_001002287	MAS-related G protein-coupled receptor, member B4	Mrgprb4	2.5	2.9
14	M64711_at	NM_080698	Fibromodulin	Fmod	1.6	2.8
15	D28860_s_at	NM_012893	Actin, gamma 2	Actg2	3.7	2.8
16	U69272_g_at	NM_017099	Potassium inwardly rectifying channel, subfamily J, member 8	Kcnj8	2.8	2.8
17	rc_AA859578_at	NM_021587	Latent transforming growth factor beta binding protein 1	Ltbp1	2.0	2.7
18	rc_AA859954_at	NM_012751	Solute carrier family 2 (facilitated glucose transporter), member 4	Slc2a4	2.3	2.7
19	rc_AI014135_g_at	NM_013113	ATPase, Na +/K + transporting, beta 1 polypeptide	Atp1b1	2.1	2.7
20	rc_AI176662_s_at	NM_019131	Tropomyosin 1, alpha	Tpm1	2.3	2.7
21	AB020504_g_at	NM_032076	Prostaglandin E receptor 4 (subtype EP4)	Ptger4	2.4	2.6
22	rc_AI232078_at	NM_012827	Bone morphogenetic protein 4	Bmp4	2.8	2.6
23	U02553cds_s_at	NM_033485	PRKC, apoptosis, WT1, regulator	Pawr	1.4	2.6
24	X63253cds_s_at	NM_080902	Hypoxia induced gene 1	Hig1	1.7	2.6
25	M60921_g_at	XR_086177	PMF32 protein (predicted)	Pmf31	2.8	2.5
26	S66024_at	XM_343144	Myosin, light polypeptide 6, alkali, smooth muscle and non-muscle (predicted)	Myl6_predicted	2.7	2.5
27	M86621_at	NM_012887	Thymopoietin	Tmpo	1.2	2.5
28	X54686cds_at/// rc_AA891041_at	XM_573030	Myosin heavy chain 11	Myh11	3.7	2.3
29	U17254_g_at	NM_012974	Laminin, beta 2	Lamb2	2.5	2.3
30	Z22607_at	NM_019620	Zinc finger protein 386 (Kruppel-like)	Znf386	7.5	2.2
31	rc_AA891422_at	NM_053650	PDZ and LIM domain 3	Pdlim3	2.6	1.8
32	rc_AI144767_s_at/// rc_AA875132_at	NM_024162	Fatty acid binding protein 3	Fabp3	3.5	1.7
33	M63656_s_at	NM_012919	Calcium channel, voltage-dependent, alpha2/delta subunit 1	Cacna2d1	2.7	1.6
34	rc_AI014163_at	NM_012548	Endothelin 1	Edn1	2.8	1.4
35	rc_AI639161_at	XM_346029	Similar to KIAA1411 protein (predicted)	RGD1304927_predicted	2.7	1.2
36	rc_AA866345_at	NM_012531	Catechol-*O*-methyltransferase	Comt	4.6	1.2
37	rc_AI230614_s_at/// rc_AI112173_at	NM_001002829	RAS-like family 11 member A	Rasl11a	3.0	1.1
38	rc_AA799511_g_at	–	–	–	1.8	2.6
39	rc_AA893871_at	–	–	–	1.4	2.5

Table 2 Aorta-dominant genes

	Probe set ID	RefSeq transcript ID	Gene title	Gene symbol	Fold difference between aorta and DA	
					e19	e21
1	X15939_r_at///rc_AI104924_f_at/// rc_AI103920_f_at///rc_AA891522_f_at	NM_017239	Myosin heavy chain, polypeptide 6, cardiac muscle, alpha	Myh6	2.2	23.8
2	X80130cds_i_at///rc_AI104567_g_at/// rc_AA866452_s_at	XM_215801	Actin alpha cardiac 1	Actc1	3.0	18.4
3	M93638_at	NM_183333	Keratin complex 2, basic, gene 5	Krt2-5	6.9	16.8
4	rc_AA891242_g_at///rc_AA891242_at	NM_001106017	Myosin, light polypeptide 7, regulatory	Myl7	3.2	15.3
5	X15939_f_at	NM_017240	Myosin, heavy polypeptide 7, cardiac muscle, beta	Myh7	1.9	13.2
6	D78159mRNA_s_at	NM_001008806	Type II keratin Kb4	Kb4	1.5	9.1
7	X15512_at	NM_012824	Apolipoprotein C–I	Apoc1	0.5	7.4
8	U67914_at	XM_342219	Carboxypeptidase A3	Cpa3	1.7	7.2
9	rc_AI169372_g_at	NM_031839	Cytochrome P450, family 2, subfamily c, polypeptide 23	Cyp2c23	0.5	5.5
10	K01933_at	NM_012582	Haptoglobin	Hp	0.5	5.1
11	M80829_at	NM_012676	Troponin T2, cardiac	Tnnt2	1.3	4.8
12	X00975_g_at///X07314cds_at	NM_001035252	Myosin, light polypeptide 2	Myl2	5.1	4.8
13	M24852_at	NM_013002	Purkinje cell protein 4	Pcp4	4.7	4.8
14	M92074_g_at	NM_017144	Troponin I, cardiac	Tnni3	2.1	4.6
15	rc_AA945054_s_at	NM_022245	Cytochrome b-5	Cyb5	0.8	4.1
16	S76779_s_at	NM_138828	Apolipoprotein E	Apoe	1.3	3.9
17	AF014503_at	NM_053611	Nuclear protein 1	Nupr1	3.2	3.9
18	X02412_at	NM_019131	Tropomyosin 1, alpha	Tpm1	1.0	3.7
19	D00752_at	NM_182474	Serine protease inhibitor	Spin2a	0.5	3.6
20	D89730_at	NM_001012039	Epidermal growth factor-containing fibulin-like extracellular matrix protein 1 (predicted)	Efemp1_predicted	4.0	3.6
21	M14656_at	NM_012881	Secreted phosphoprotein 1	Spp1	4.7	3.4
22	X81448cds_at///rc_AI072634_at	NM_053976	Keratin complex 1, acidic, gene 18	Krt1-18	1.5	3.1
23	rc_AA946368_at	XM_575338	Similar to fatty acid translocase/CD36	LOC499984	1.9	3.1
24	M91595exon_s_at///J04486_at/// A09811cds_s_at	NM_013122	Insulin-like growth factor binding protein 2	Igfbp2	2.1	3.1
25	U30938_at	NM_013066	Microtubule-associated protein 2	Mtap2	2.1	3.0
26	Y12502cds_at	NM_021698	Coagulation factor XIII, A1 subunit	F13a	2.8	2.9
27	M84719_at	NM_012792	Flavin containing monooxygenase 1	Fmo1	4.4	2.8
28	M91652complete_seq_at	NM_017073	Glutamine synthetase 1	Glul	1.8	2.8
29	J03752_at	NM_134349	Microsomal glutathione *S*-transferase 1	Mgst1	1.1	2.7
30	AF072411_g_at///rc_AA925752_at	NM_031561/// XM_575338/// XM_575339	CD36 antigen///similar to fatty acid translocase/CD36///similar to fatty acid translocase/CD36	Cd36///LOC499984/// LOC499985	1.7	2.7
31	L19998_g_at///L19998_at	NM_031834	Sulfotransferase family 1A, phenol-preferring, member 1	Sult1a1	2.9	2.7
32	L25387_g_at	NM_206847	Phosphofructokinase, platelet	Pfkp	1.7	2.6
33	rc_AI230247_s_at	NM_019192	Selenoprotein P, plasma, 1	Sepp1	2.2	2.6
34	rc_AI237731_s_at///L03294_g_at///L03294_at	NM_012598	Lipoprotein lipase	Lpl	0.9	2.6
35	M83680_at	NM_053589	RAB14, member RAS oncogene family	Rab14	2.6	2.6
36	rc_AI639532_at	XM_215935	Troponin C2, fast (predicted)	Tnnc2_predicted	4.7	2.5
37	X71127_g_at	NM_019262	Complement component 1, q subcomponent, beta polypeptide	C1qb	3.2	2.5
38	AB000113_at	NM_017217	Solute carrier family 7 (cationic amino acid transporter, y + system), member 3	Slc7a3	1.6	2.5
39	rc_AA894092_at	XM_342245	Periostin, osteoblast specific factor (predicted)	Postn_predicted	2.5	2.5
40	M32062_g_at	NM_053843/// XM_573502/// XM_573503	Fc receptor, IgG, low affinity III///Fc gamma receptor II beta///similar to low affinity immunoglobulin gamma Fc region receptor III precursor (IgG Fc receptor III) (Fc-gamma RIII) (FcRIII)	Fcgr3/// LOC498276/// LOC498277	3.2	2.4
41	M24353_g_at	XM_343636	Mannosidase 2, alpha 1	Man2a1	4.7	2.3

Table 2 continued

	Probe set ID	RefSeq transcript ID	Gene title	Gene symbol	Fold difference between aorta and DA	
					e19	e21
42	U77931_at	NM_147136	rRNA promoter binding protein	RGD:727924	3.0	2.3
43	M12098_s_at	NM_012604	Myosin, heavy polypeptide 3, skeletal muscle, embryonic	Myh3	2.7	2.1
44	AJ005396_at	XM_342325	Procollagen, type XI, alpha 1	Col11a1	3.1	2.1
45	rc_AA893230_at	XM_236325	Ceroid-lipofuscinosis, neuronal 6 (predicted)	Cln6_predicted	2.8	2.1
46	rc_AA875172_at	NM_053360	SH3-domain kinase binding protein 1	Sh3kbp1	2.6	2.1
47	AB012235_at///AB012234_g_at/// AB012234_at	XM_213849	Nuclear factor I/X	Nfix	4.9	1.9
48	X00722_at	XM_578812	Similar to testin	LOC503278	2.8	1.9
49	M32062_at	NM_053843/// XM_573502	Fc receptor, IgG, low affinity III///Fc gamma receptor II beta	Fcgr3///LOC498276	2.8	1.8
50	rc_AI013472_at///rc_AA924925_at	NM_138905	ER transmembrane protein Dri 42	Ppap2b	2.6	1.8
51	U62897_at	NM_012836	Carboxypeptidase D	Cpd	3.0	1.8
52	Z12298cds_s_at///X59859_r_at///X59859_i_at	NM_024129	Decorin	Dcn	2.7	1.7
53	M15797_at	XM_213954	Nidogen (entactin)	Nid	13.4	1.7
54	AF041066_at	NM_020082	Ribonuclease, RNase A family 4	Rnase4	2.9	1.7
55	U50842_at	XM_343427	Neural precursor cell expressed, developmentally downregulated gene 4A	Nedd4a	3.9	1.6
56	rc_AA866443_at	NM_001008560	Protease, serine, 35 (predicted)	Prss35	4.2	1.6
57	S66184_s_at///rc_AI234060_s_at/// rc_AI102814_at///rc_AA875582_at	NM_017061	Lysyl oxidase	Lox	3.2	1.6
58	rc_AI639314_at	XM_238213	Delangin (predicted)	NIPBL_predicted	2.5	1.6
59	rc_AA800908_at	XM_344450	Potassium channel tetramerisation domain containing 12 (predicted)	Kctd12_predicted	3.6	1.6
60	rc_AI029920_s_at	NM_012817	Insulin-like growth factor binding protein 5	Igfbp5	4.0	1.5
61	L10326_at	NM_019132	GNAS complex locus	Gnas	2.7	1.5
62	E00988mRNA_s_at	NM_031511	Insulin-like growth factor 2	Igf2	3.0	1.4
63	U01908cds_s_at///D43778exon#3_s_at/// D16840_s_at	NM_012494	Angiotensin II receptor, type 2	Agtr2	4.4	1.4
64	rc_AI176461_s_at	NM_017211	Golgi apparatus protein 1	Glg1	3.3	1.4
65	U23146cds_s_at	NM_057103	A kinase (PRKA) anchor protein (gravin) 12	Akap12	2.9	1.4
66	rc_AA900750_s_at	NM_012760	Pleiomorphic adenoma gene-like 1	Plagl1	2.5	1.4
67	Z17223_at	NM_017149	Mesenchyme homeo box 2	Meox2	2.6	1.3
68	rc_AI171966_at	NM_198740	Major histocompatibility complex, class II, DM beta	RGD:735096	2.5	1.2
69	U35775_g_at///U35775_at	NM_031552	Adducin 3 (gamma)	Add3	5.3	1.2
70	U43534_at	NM_012894	Adenosine deaminase, RNA-specific, B1	Adarb1	2.7	0.8
71	AF004811_at	NM_030863	Moesin	Msn	2.9	0.7
72	X05831cds_at///U82612cds_at///M28259cds_at	NM_019143	Fibronectin 1	Fn1	3.9	0.7
73	U17604_at	NM_053865	Reticulon 1	Rtn1	2.6	0.7
74	X51531cds_g_at///X51531cds_at	–	–	–	4.4	30.2
75	rc_AA799865_at	–	Transcribed locus	–	1.3	2.7
76	X05472cds#2_at	–	–	–	7.2	2.4
77	rc_AA799406_at	XM_578859	Hypothetical protein LOC503325	LOC503325	2.6	1.3
78	rc_AA859921_at	–	–	–	3.3	0.9

in the aorta at e19 and at e21 ($p < 0.05$ and $p < 0.001$, $n = 6$–8, respectively) (Fig. 2a).

We then examined the localization of GHR in the DA and the aorta at e19 and e21. GHR immunoreactivity was detected abundantly in the SMC layer and less in the endothelial cells of the DA (Fig. 2b).

GH promoted DA SMC migration, but not proliferation

SMC migration and proliferation play an essential role in intimal cushion formation of the DA, especially during late gestation. Therefore, we investigated the effects of GH on migration and proliferation using DA SMCs in primary

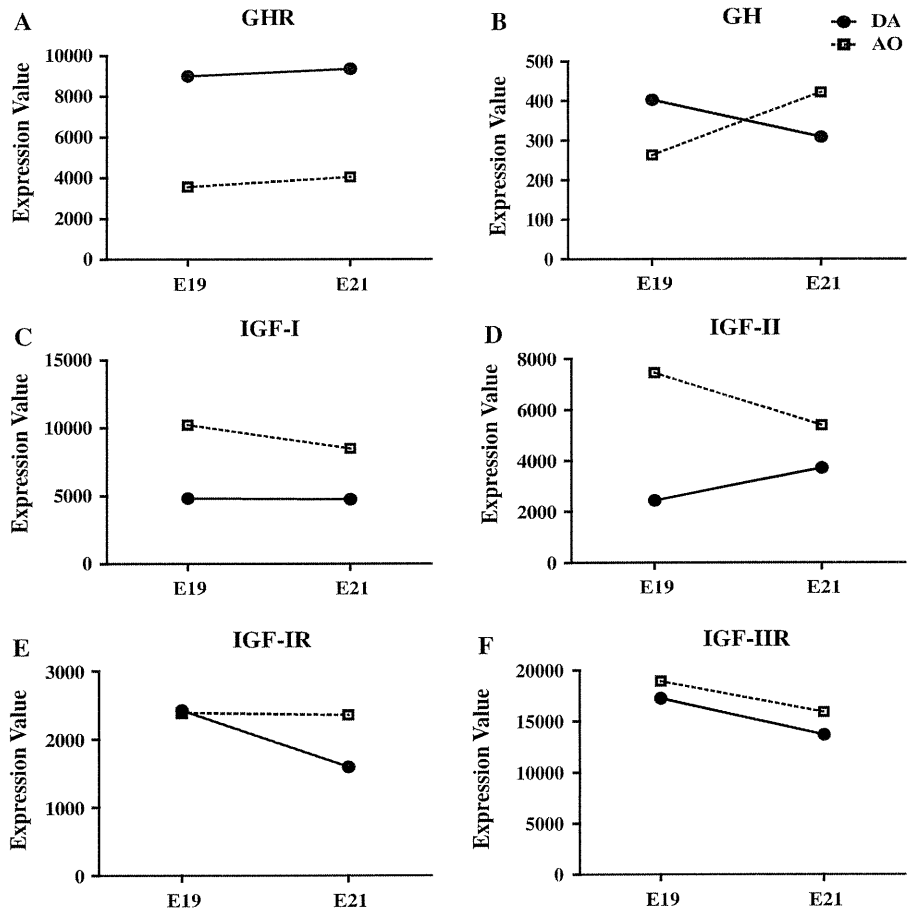

Fig. 1 The expression of growth hormone receptor and its related genes in the developing DA by DNA microarray analysis. **a** GHR (growth hormone receptor), **b** GH (growth hormone), **c** IGF (insulin-like growth factor)-I, **d** IGF-II, **e** IGF-IR (type I receptor), and **f** IGF-IIR (type II receptor) mRNA. *E19* Embryonic day 19, *E21* embryonic day 21, *DA* ductus arteriosus, *AO* aorta

culture from rat DA at e21. We found that recombinant rat GH promoted migration of DA SMCs in a dose-dependent manner (Fig. 3a). However, the same amount of GH did not promote migration of aortic SMCs (Supplemental data 3). When DA SMCs were treated with platelet-derived growth factor BB (PDGF-BB) (10 ng/ml), a potent stimulator for SMC migration, SMC migration was significantly increased by 141% in DA SMCs. In contrast, [^{3}H]thymidine incorporation was unchanged in DA SMCs in the presence of recombinant rat GH (up to 200 ng/ml) (Fig. 3b). When DA SMCs were treated with 10% FBS, a potent stimulator for SMC proliferation, [^{3}H]thymidine incorporation was significantly increased by 112% in DA SMCs. Hyaluronan is an important component of the intimal cushion, and hyaluronan-rich matrices are essential for cell migration and proliferation in the DA [2]. Because our recent study revealed that PGE_1 is a potent stimulator for hyaluronan production in DA SMCs [2], we investigated whether or not GH altered hyaluronan production in DA SMCs. We found that GH had no effect on hyaluronan production in DA SMCs (data not shown).

Effect of GH on tissue-specific cytoskeletal genes in the DA and the aorta

Our DNA array analyses revealed that the expression of cytoskeletal genes was markedly different between the DA and the aorta. Because GH is known to regulate cytoskeletal organization [7], we examined whether or not GH affected such a tissue-specific expression of cytoskeletal genes in DA SMCs. We found that GH decreased the expression of DA-dominant cytoskeletal genes such as desmin, Fhl2, Actg2, and Myh11 in DA SMCs (Fig. 4a–d). Among the aorta-dominant sarcomere genes, we also found that GH decreased the expression of Myl2 and Tnnt2 mRNAs, increased the expression of Tnni3 mRNA, and exhibited no change in Myh7, Actc1, and Tnnc2 mRNAs (Fig. 5).

Because GH is known to inhibit the expression of skeletal muscle-specific proteins in a dose-dependent manner in satellite cells [8], we examined the effect of GH on the expression of smooth muscle-specific genes. We found that GH significantly decreased the expression of SM1, SM2, SM22, and h-caldesmon mRNAs, whereas GH did not

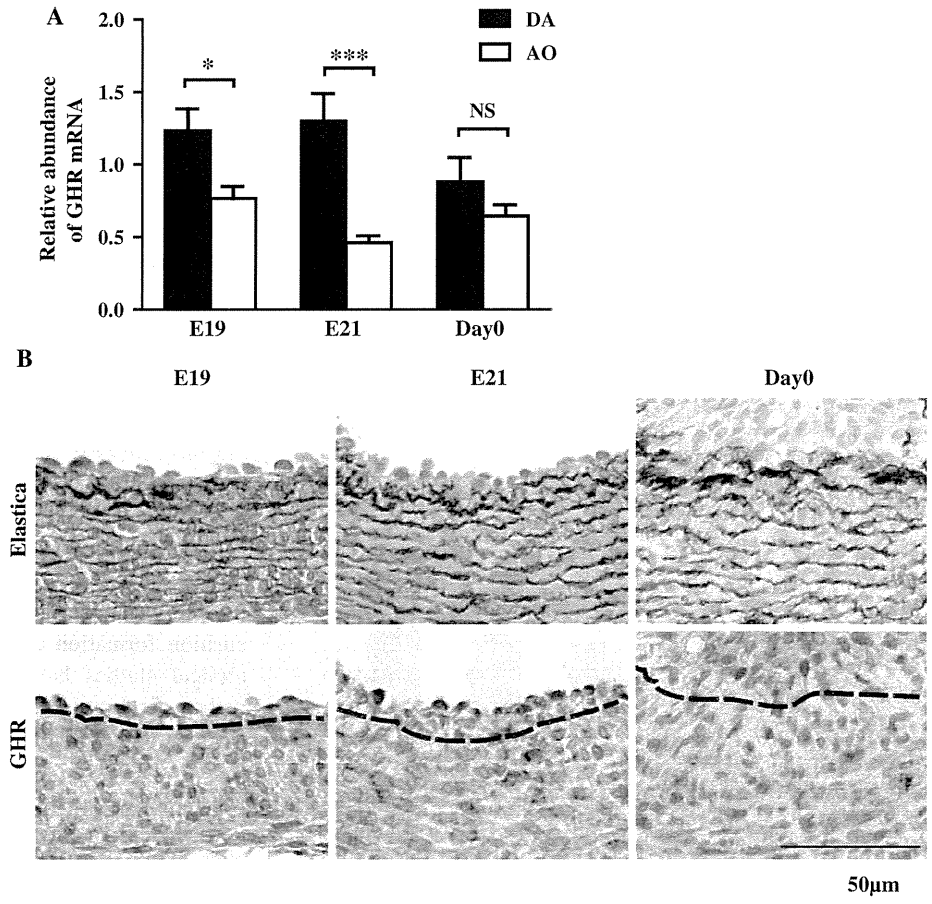

Fig. 2 Expression of GHR mRNA and protein in rat DA. **a** Quantitative RT-PCR analyses of GHR. The expression level of GHR mRNA was maximal at E19 and E21 in the DA ($n = 6$–8). **b** Immunohistological analysis of GHR protein in the rat DA at E19, E21, and Day0. GHR was detected in a *brown color*. Dark blue stain was counterstained with Mayer's hematoxylin. *Scale bars* 50 mm. $*p < 0.05$, $***p < 0.001$. Data are expressed as means ± SEM. *E19* Embryonic day 19, *E21* embryonic day 21, *Day0* at birth, *DA* ductus arteriosus, *AO* aorta, *GHR* growth hormone receptor, *NS* not significant

change the expression of SMemb mRNA (Fig. 6a–e). We also found that GH decreased the expression of myocardin mRNA (Fig. 6f), a transcriptional factor, which is sufficient for a smooth muscle-like contractile phenotype. To investigate whether the effect of GH on the expression of cytoskeletal genes is found in aortic SMCs, we also did the same experiment using SMCs from the rat aorta at e21. We also found a similar effect of GH on the expression of cytoskeletal genes in cultured rat aortic SMCs (Supplemental data 4, 5, and 6).

GH promoted intimal thickening of immature rat DA explants

To examine to what extent GH contributes to the intimal thickening of the DA, we administrated GH into the premature vessel explants containing the DA, the aorta, and the main pulmonary artery from fetuses at e19 (Fig. 7). We found that GH significantly promoted intimal thickening of the DA, but not the aorta when compared with the control (Fig. 7). It should be noted that the effect of GH on the intimal thickening was greater in the DA than in the aorta.

Discussion

Our microarray analyses uncovered gene expression profiles of the DA distinct from those of the aorta during fetal development. These gene expression profiles are considered to be the primary determinant of the different functional and morphological characteristics of the DA from the adjacent arteries. In fact, several unexpected genes that are known to be involved in tissue differentiation were identified as having a DA-dominant expression pattern. It is of note that among them GHR exhibited the highest difference in expression between the rat developing DA and the adjacent aorta. Although the expression levels of GH mRNA were slightly higher in the aorta than in the DA at e21, the difference did not reach statistical significance. We think that total GH-GHR signals are higher in the DA than in the aorta due to the predominant expression of GHR in the DA during gestation. Accordingly, we hypothesized that GH stimulation via GHR may be involved in DA remodeling and that it may play a role in the specification of the DA from other arteries. During gestation, the serum GH concentration of fetuses increased gradually as

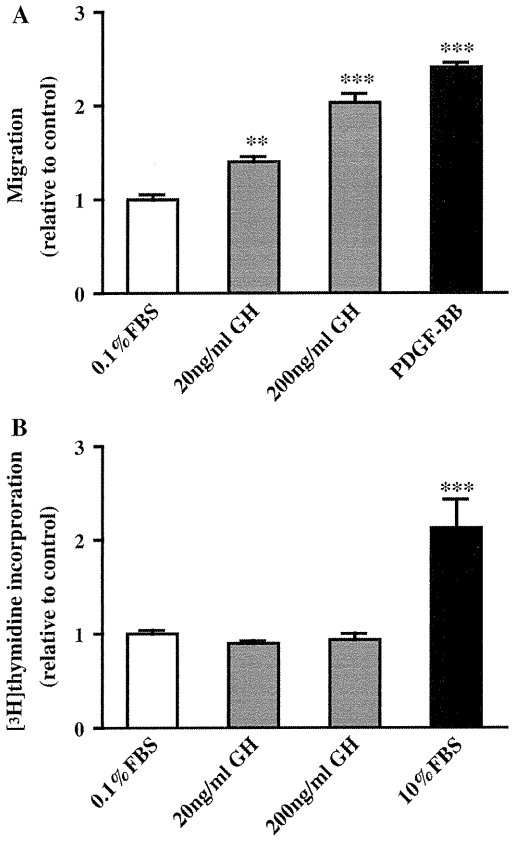

Fig. 3 GH promoted DA SMC migration, but not proliferation. **a** Effects of growth hormone (GH) stimulation on DA SMC migration. DA SMC migration was significantly increased in the presence of GH at a concentration of 20 or 200 ng/ml ($n = 6$). PDGF-BB at a concentration of 10 ng/ml was used as a positive control. **b** The effect of GH on proliferation of rat DA SMCs. GH did not promote cell proliferation in DA SMCs ($n = 6$–8); 10% FBS was used as a positive control. $^{**}p < 0.01$,$^{***}p < 0.001$ versus 0.1% FBS. Data are expressed as means ± SEM. *FBS* Fetal bovine serum

pregnancy advanced and declined before parturition in many species [9–11]. In rodents, the fetal pituitary gland starts to secret GH from e15, whereas many tissues, including vascular endothelial and SMCs, locally produce GH beginning in relatively early embryogenesis [12]. Even though the level of serum GH in a fetus is almost comparable to or slightly less than that in an adolescenct [9–11], GH has been regarded as of little functional significance in fetal growth [13]. A growing body of evidence, however, has revealed the importance of GH in tissue differentiation during fetal development. First, many fetal tissues, including vascular endothelium and smooth muscle, express GHR [14, 15]. Therefore, GH likely activates an intracellular signal pathway through GHR in fetuses. Second, a considerable number of studies have demonstrated that fetal tissues indeed respond to GH in vitro [12, 16], which was observed in the present study. Third, GHR knockout mice exhibit functional and morphological changes in both heart and vasculature [17]. These results led us to explore the role of GH in DA development, especially in its vascular remodeling.

Numerous previous studies have demonstrated that GH plays a role in angiogenesis [18] and that GH deficiency or excess increases the risk of cardiovascular morbidity and mortality [19, 20]. However, the role of GH in the vascular remodeling of the developmental arteries has not yet been precisely evaluated. The present study revealed that GH promoted the migration of DA SMCs and then intimal cushion formation in DA explants. In terms of the effect of GH on SMC migration, data from previous studies are very limited [21–23]. Although the precise mechanism still has not been investigated, it can be assumed that the different responses to GH in various cell types are dependent on the GHR expression levels.

Intimal thickness is a hallmark of physiological vascular remodeling of the DA during late gestation [2]. Although the present study demonstrated that GH promotes intimal cushion formation of the ex vivo DA explants, previous clinical studies have shown that the effect of GH on pathological intimal thickness is equivocal. Increases in the carotid intimal media thickness were observed in patients with acromegaly [24]. In contrast, patients with either childhood- or adulthood-onset GH deficiency also exhibited increased intima-media thickness and endothelial dysfunction [19, 25]. Therefore, adequate levels of GH could be important to maintain normal morphology of mature arteries. The present study indicates that GH in the culture media at a concentration of 200 ng/ml is sufficient to promote the physiological intimal cushion formation of the DA through increasing SMC migration.

It is known that the differentiation of DA SMCs precedes that of other arteries [26, 27]. Nevertheless, we were surprised by the considerable number of cardiac-type sarcomere genes expressed in the fetal DA, although it was much less than that in the aorta. The present data suggest that prior to complete differentiation, vascular SMCs may retain a high degree of plasticity, which allows them to modulate their phenotype [28]. Interestingly, through the in vitro experiment, we found that the effect of GH on the expression of the cytoskeletal genes was not always consistent with the tissue-dominant expression patterns that were identified by DNA microarray analysis. Therefore, factor(s) other than GH may determine the tissue-specific expression pattern of cytoskeletal genes in the DA and the aorta.

More importantly, we found that GH downregulated the genes involved in a smooth muscle-like contractile phenotype. Consistent with the result, we also found that GH downregulated myocardin mRNA, which is sufficient for a smooth muscle-like contractile phenotype [28]. In addition

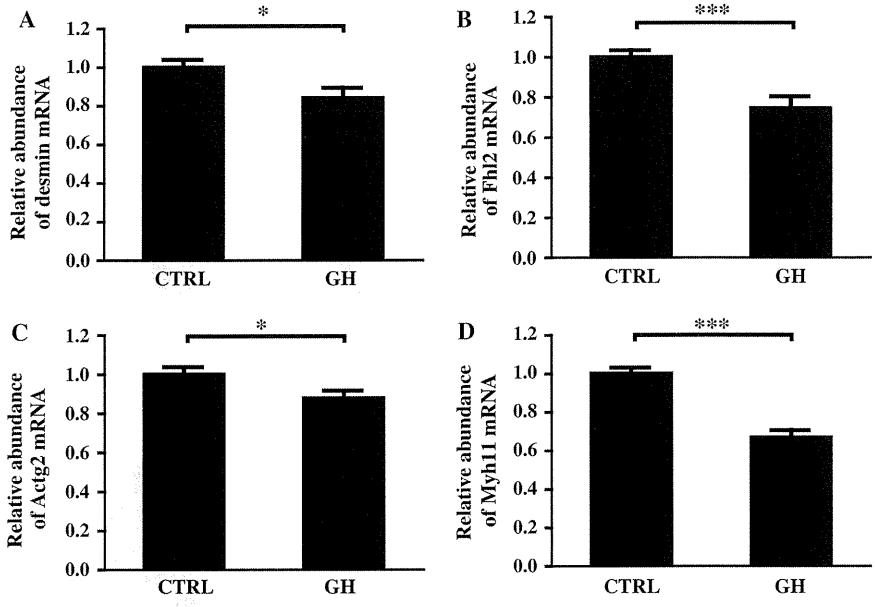

Fig. 4 Effect of GH on the cytoskeletal genes and smooth muscle-specific genes in DA SMCs. **a** Desmin, **b** Fhl2, **c** Actg2, **d** Myh11. ($n = 15$). $*p < 0.05$, $***p < 0.001$. Data are expressed as means ± SEM. *GH* Growth hormone, *CTRL* control, *DA SMC* ductus arteriosus smooth muscle cell, *NS* not significant

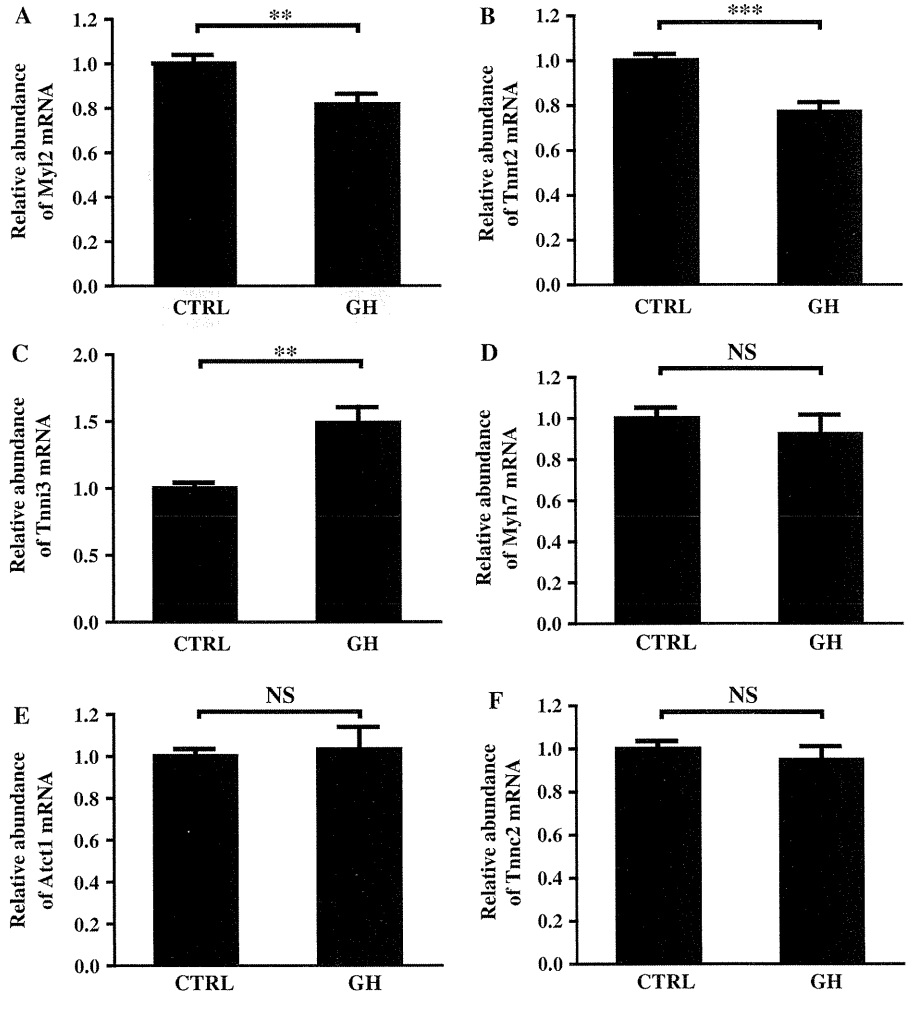

Fig. 5 Effect of GH on the expression of the aorta-dominant sarcomere genes in DA SMCs. **a** Myl2, **b** Tnnt2, **c** Tnni3, **d** Myh7, **e** Actc1, and **f** Tnnc2. ($n = 15$). $**p < 0.01$, $***p < 0.001$. Data are expressed as means ± SEM. *GH* Growth hormone, *CTRL* control, *DA SMC* ductus arteriosus smooth muscle cell, *NS* not significant

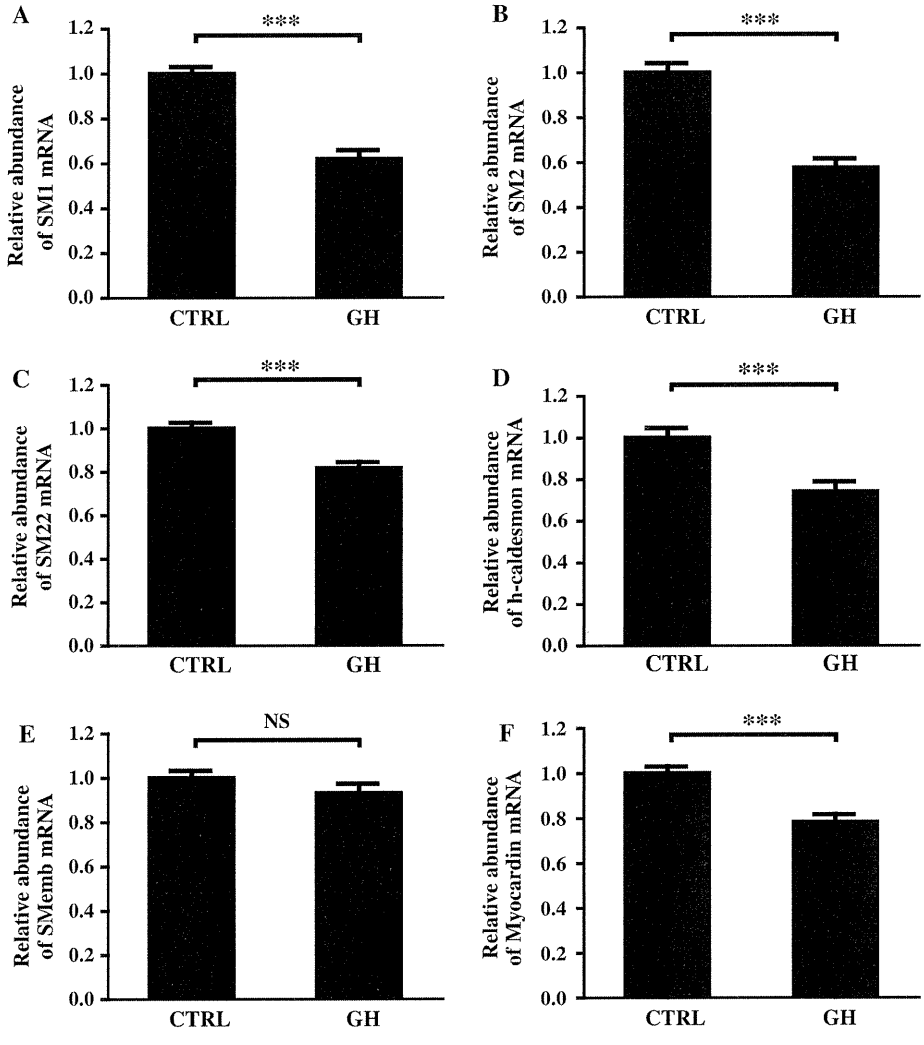

Fig. 6 Effect of GH on the cytoskeletal genes and smooth muscle-specific genes in DA SMCs. **a** SM1, **b** SM2, **c** SM22, **d** h-caldesmon, **e** SMemb, **f** Myocardin. ($n = 15$). $^{*}p < 0.05$, $^{***}p < 0.001$. Data are expressed as means ± SEM. *GH* Growth hormone, *CTRL* control, *DA SMC* ductus arteriosus smooth muscle cell, *NS* not significant

to this observation, Halevy et al. [8] demonstrated that GH inhibited the gene expression of myogenin and the expression of skeletal muscle-specific proteins in a dose-dependent manner in satellite cells. These data suggested that during muscle differentiation, GH inhibited the muscle-specific differentiation at its final stage to retain its synthetic phenotype. We propose that DA SMCs consist of distinct types that depend on their localization. During the progression of intimal cushion formation, DA SMCs in the inner layer are a synthetic phenotype that is highly proliferative and can migrate easily. The GH-GHR signal helps these cells remain a synthetic phenotype. Further studies are required to prove this idea.

Although the present microarray analyses uncovered distinct gene expression profiles of the DA from those of the aorta, several gene profiles are different from a previous report demonstrating the transcriptional profiles between the rat DA and the aorta of premature fetuses and neonates using the same DNA microarray plates we used [3]. For example, Costa et al. demonstrated that Myl2 and Myh7 are predominantly expressed in the rat aorta at e19, but our data showed the opposite result. In addition, the tissue-specific genes that we identified overlap very little with their findings. We do not have a reasonable explanation for this discrepancy. It should be noted that the present study identified several expected genes that are known to be predominantly expressed in the DA, such as prostaglandin E receptor 4, endothelin-1, and Kcnj8 (potassium inwardly rectifying channel, subfamily J, member 8). In contrast, Costa et al. did not identify this expected DA-dominant gene in the data from their microarray analysis. Furthermore, we also confirmed by quantitative RT-PCR analysis that, using different sets of RNA samples, the expression of several DA-dominant genes was higher in the DA than in the aorta. Therefore, we are confident that we provided

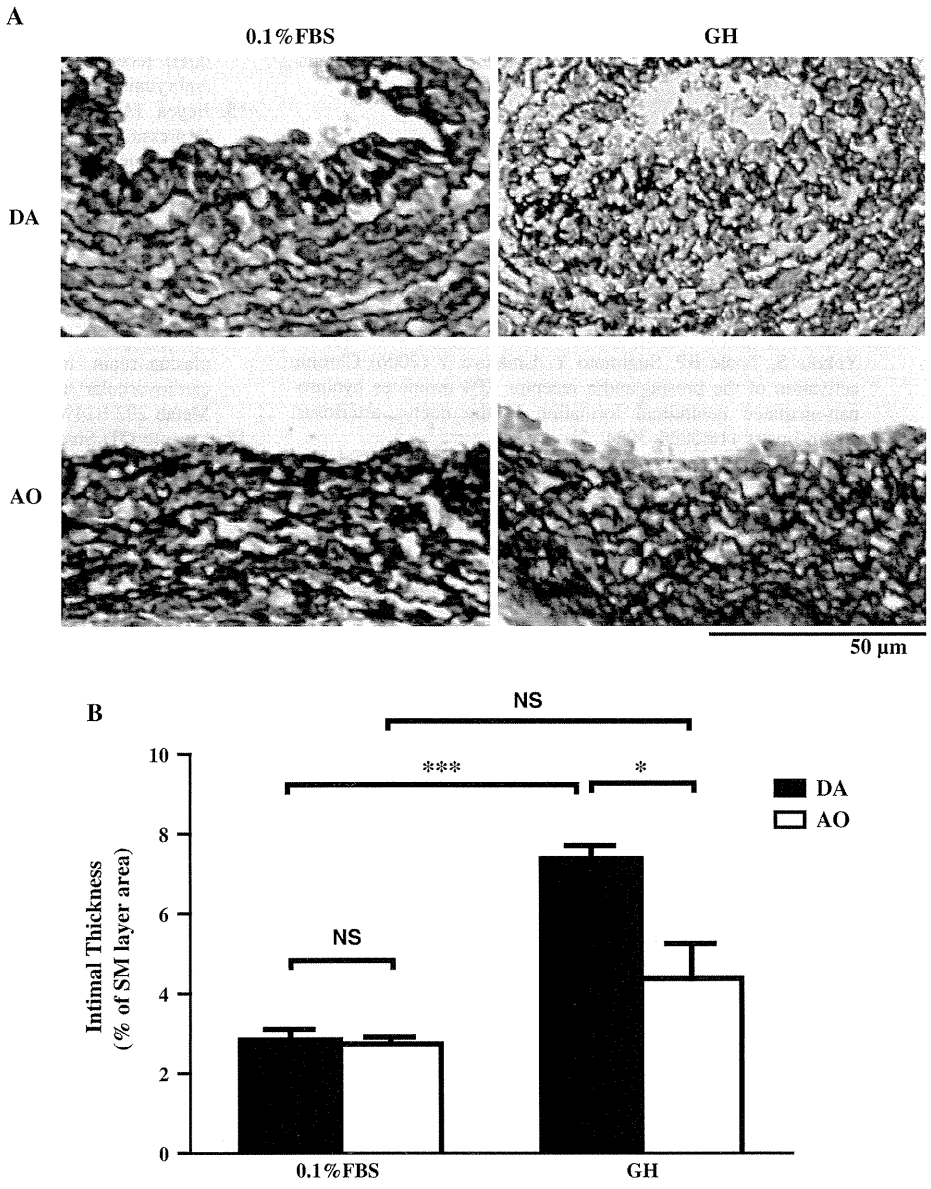

Fig. 7 Effects of GH-mediated intimal thickening of immature rat DA and aorta explants. **a** Elastica staining of the DA and the aorta. GH at a concentration of 200 ng/ml. *Scale bars* 50 μm. **b** GH significantly promoted intimal thickening of the DA, but not the aorta. ($n = 4$–6). $^{*}p < 0.05$,$^{***}p < 0.001$. Data are expressed as means ± SEM. *DA* Ductus arteriosus, *AO* aorta, *GH* growth hormone, *NS* not significant

reliable data regarding the transcriptional profiles of the developing rat DA.

In conclusion, our study highlighted the distinct transcriptional profiles of the DA. In addition to the expected genes, microarray analysis revealed many genes whose roles were previously unrecognized in the DA. Among them, we found that the GH-GHR signal plays a role in vascular remodeling of the DA by promoting migration of SMCs and the subsequent formation of intimal thickness and regulating the expression of cytoskeletal genes. Although further studies are needed to identify the role of other genes in the DA, our data provide a basis for understanding the molecular mechanisms underlying the differentiation and remodeling of the DA and for inventing the novel targets that regulate the contraction of the DA in affected children.

Acknowledgments This work was supported by grants from the Ministry of Health Labor and Welfare (Y.I.), the Ministry of Education, Culture, Sports, Science, and Technology of Japan (Y.I., U.Y., S.M.), the Foundation for Growth Science (S.M.), the Yokohama Foundation for Advanced Medical Science (U.Y., S.M.), the 'High-Tech Research Center' Project for Private Universities: MEXT (S.M.), a Waseda University Grant for Special Research Projects (Q.J.), the Vehicle Racing Commemorative Foundation (S.M.), Miyata Cardiology Research Promotion Funds (U.Y., S.M.), Takeda Science Foundation (Y.I., U.Y., S.M.), the Japan Heart Foundation Research Grant (U.Y.), the Kowa Life Science Foundation (U.Y.),

the Sumitomo Foundation (U.Y), Japan Cardiovascular Research Foundation (S.M.), Mochida Memorial Foundation for Medical and Pharmaceutical Research (U.Y.) and the Uehara Memorial Foundation (U.Y.).

References

1. Smith GC (1998) The pharmacology of the ductus arteriosus. Pharmacol Rev 50:35–58
2. Yokoyama U, Minamisawa S, Quan H, Ghatak S, Akaike T, Segi-Nishida E, Iwasaki S, Iwamoto M, Misra S, Tamura K, Hori H, Yokota S, Toole BP, Sugimoto Y, Ishikawa Y (2006) Chronic activation of the prostaglandin receptor EP4 promotes hyaluronan-mediated neointimal formation in the ductus arteriosus. J Clin Invest 116:3026–3034
3. Costa M, Barogi S, Socci ND, Angeloni D, Maffei M, Baragatti B, Chiellini C, Grasso E, Coceani F (2006) Gene expression in ductus arteriosus and aorta: comparison of birth and oxygen effects. Physiol Genomics 25:250–262
4. Yokoyama U, Sato Y, Akaike T, Ishida S, Sawada J, Nagao T, Quan H, Jin M, Iwamoto M, Yokota S, Ishikawa Y, Minamisawa S (2007) Maternal vitamin A alters gene profiles and structural maturation of the rat ductus arteriosus. Physiol Genomics 31:139–157
5. Akaike T, Jin MH, Yokoyama U, Izumi-Nakaseko H, Jiao Q, Iwasaki S, Iwamoto M, Nishimaki S, Sato M, Yokota S, Kamiya Y, Adachi-Akahane S, Ishikawa Y, Minamisawa S (2009) T-type Ca2+ channels promote oxygenation-induced closure of the rat ductus arteriosus not only by vasoconstriction but also by neointima formation. J Biol Chem 284:24025–24034
6. Yokoyama U, Minamisawa S, Katayama A, Tang T, Suzuki S, Iwatsubo K, Iwasaki S, Kurotani R, Okumura S, Sato M, Yokota S, Hammond HK, Ishikawa Y (2010) Differential regulation of vascular tone and remodeling via stimulation of type 2 and type 6 adenylyl cyclases in the ductus arteriosus. Circ Res 106:1882–1892
7. Florini JR, Ewton DZ, Coolican SA (1996) Growth hormone and the insulin-like growth factor system in myogenesis. Endocr Rev 17:481–517
8. Halevy O, Hodik V, Mett A (1996) The effects of growth hormone on avian skeletal muscle satellite cell proliferation and differentiation. Gen Comp Endocrinol 101:43–52
9. Kishi K, Hirashiba M, Hasegawa Y (1991) Gestational profiles of rat placental lactogen-II (rPL-II) and growth hormone (GH) in maternal and fetal serum, amniotic fluid, and placental tissue. Endocrinol Jpn 38:589–595
10. Bassett JM, Thorburn GD, Wallace AL (1970) The plasma growth hormone concentration of the foetal lamb. J Endocrinol 48:251–263
11. Kaplan SL, Grumbach MM, Shepard TH (1972) The ontogenesis of human fetal hormones I. Growth hormone and insulin. J Clin Invest 51:3080–3093
12. Waters MJ, Kaye PL (2002) The role of growth hormone in fetal development. Growth Horm IGF Res 12:137–146
13. Gluckman PD, Grumbach MM, Kaplan SL (1981) The neuroendocrine regulation and function of growth hormone and prolactin in the mammalian fetus. Endocr Rev 2:363–395
14. Garcia-Aragon J, Lobie PE, Muscat GE, Gobius KS, Norstedt G, Waters MJ (1992) Prenatal expression of the growth hormone (GH) receptor/binding protein in the rat: a role for GH in embryonic and fetal development? Development 114:869–876
15. Beyea JA, Olson DM, Vandergriend RA, Harvey S (2005) Expression of growth hormone and its receptor in the lungs of embryonic chicks. Cell Tissue Res 322:379–392
16. Giustina A, Mazziotti G, Canalis E (2008) Growth hormone, insulin-like growth factors, and the skeleton. Endocr Rev 29:535–559
17. Egecioglu E, Andersson IJ, Bollano E, Palsdottir V, Gabrielsson BG, Kopchick JJ, Skott O, Bie P, Isgaard J, Bohlooly YM, Bergstrom G, Wickman A (2007) Growth hormone receptor deficiency in mice results in reduced systolic blood pressure and plasma renin, increased aortic eNOS expression, and altered cardiovascular structure and function. Am J Physiol Endocrinol Metab 292:E1418–E1425
18. Lincoln DT, Singal PK, Al-Banaw A (2007) Growth hormone in vascular pathology: neovascularization and expression of receptors is associated with cellular proliferation. Anticancer Res 27:4201–4218
19. Klibanski A (2003) Growth hormone and cardiovascular risk markers. Growth Horm IGF Res 13(Suppl A):S109–S115
20. Colao A (2008) The GH-IGF-I axis and the cardiovascular system: clinical implications. Clin Endocrinol (Oxf) 69:347–358
21. Schultz K, Rasmussen LM, Ledet T (2005) Expression levels and functional aspects of the hyaluronan receptor CD44. Effects of insulin, glucose, IGF-I, or growth hormone on human arterial smooth muscle cells. Metabolism 54:287–295
22. Ikeo S, Yamauchi K, Shigematsu S, Nakajima K, Aizawa T, Hashizume K (2001) Differential effects of growth hormone and insulin-like growth factor I on human endothelial cell migration. Am J Physiol Cell Physiol 280:C1255–C1261
23. Lee SW, Kim SH, Kim JY, Lee Y (2010) The effect of growth hormone on fibroblast proliferation and keratinocyte migration. J Plast Reconstr Aesthet Surg 63:e364–e369
24. Colao A, Spiezia S, Cerbone G, Pivonello R, Marzullo P, Ferone D, Di Somma C, Assanti AP, Lombardi G (2001) Increased arterial intima-media thickness by B-M mode echodoppler ultrasonography in acromegaly. Clin Endocrinol (Oxf) 54:515–524
25. Pfeifer M, Verhovec R, Zizek B, Prezelj J, Poredos P, Clayton RN (1999) Growth hormone (GH) treatment reverses early atherosclerotic changes in GH-deficient adults. J Clin Endocrinol Metab 84:453–457
26. Kim HS, Aikawa M, Kimura K, Kuro-o M, Nakahara K, Suzuki T, Katoh H, Okamoto E, Yazaki Y, Nagai R (1993) Ductus arteriosus. Advanced differentiation of smooth muscle cells demonstrated by myosin heavy chain isoform expression in rabbits. Circulation 88:1804–1810
27. Colbert MC, Kirby ML, Robbins J (1996) Endogenous retinoic acid signaling colocalizes with advanced expression of the adult smooth muscle myosin heavy chain isoform during development of the ductus arteriosus. Circ Res 78:790–798
28. Kumar MS, Owens GK (2003) Combinatorial control of smooth muscle-specific gene expression. Arterioscler Thromb Vasc Biol 23:737–747

THE JOURNAL OF BIOLOGICAL CHEMISTRY VOL. 286, NO. 20, pp. 17766–17776, May 20, 2011

Identification of Transcription Factor E3 (TFE3) as a Receptor-independent Activator of $G\alpha_{16}$

GENE REGULATION BY NUCLEAR Gα SUBUNIT AND ITS ACTIVATOR[*][S]

Received for publication, January 8, 2011, and in revised form, March 7, 2011 Published, JBC Papers in Press, March 24, 2011, DOI 10.1074/jbc.M111.219816

Motohiko Sato[‡1], Masahiro Hiraoka[‡], Hiroko Suzuki[‡], Yunzhe Bai[‡], Reiko Kurotani[‡], Utako Yokoyama[‡], Satoshi Okumura[‡], Mary J. Cismowski[§], Stephen M. Lanier[¶], and Yoshihiro Ishikawa[‡2]

From the [‡]Cardiovascular Research Institute, Yokohama City University School of Medicine, Fukuura, Yokohama 236-0004, Japan, [§]Center for Cardiovascular and Pulmonary Research, Research Institute at Nationwide Children's Hospital, Columbus, Ohio 43205, and [¶]Department of Pharmacology, Medical University of South Carolina, Charleston, South Carolina 29425

Receptor-independent G-protein regulators provide diverse mechanisms for signal input to G-protein-based signaling systems, revealing unexpected functional roles for G-proteins. As part of a broader effort to identify disease-specific regulators for heterotrimeric G-proteins, we screened for such proteins in cardiac hypertrophy using a yeast-based functional screen of mammalian cDNAs as a discovery platform. We report the identification of three transcription factors belonging to the same family, transcription factor E3 (TFE3), microphthalmia-associated transcription factor, and transcription factor EB, as novel receptor-independent activators of G-protein signaling selective for $G\alpha_{16}$. TFE3 and $G\alpha_{16}$ were both up-regulated in cardiac hypertrophy initiated by transverse aortic constriction. In protein interaction studies *in vitro*, TFE3 formed a complex with $G\alpha_{16}$ but not with $G\alpha_{i3}$ or $G\alpha_s$. Although increased expression of TFE3 in heterologous systems had no influence on receptor-mediated $G\alpha_{16}$ signaling at the plasma membrane, TFE3 actually translocated $G\alpha_{16}$ to the nucleus, leading to the induction of claudin 14 expression, a key component of membrane structure in cardiomyocytes. The induction of claudin 14 was dependent on both the accumulation and activation of $G\alpha_{16}$ by TFE3 in the nucleus. These findings indicate that TFE3 and $G\alpha_{16}$ are up-regulated under pathologic conditions and are involved in a novel mechanism of transcriptional regulation via the relocalization and activation of $G\alpha_{16}$.

Heterotrimeric G-proteins play key roles in transducing cell surface stimuli to intracellular signaling events (1, 2). Activation of G-protein coupled receptors (GPCRs)[3] at the cell surface initiates nucleotide exchange on Gα subunits, leading to a conformational change in $G\alpha\beta\gamma$ and subsequent transduction of signals to various intracellular effector molecules. In addition to the basic components of the G-protein signaling system (*i.e.* GPCRs, heterotrimeric G-proteins, and effector molecules), there is a novel class of regulatory proteins for heterotrimeric G-proteins that directly regulate the activation status of heterotrimeric G-proteins independently of GPCRs (3–10).

Such receptor-independent G-protein regulators are involved in unexpected and important functional roles of heterotrimeric G-proteins in multiple cellular events. For example, LGN (activator of G-protein signaling 5 (AGS5)) and AGS3 are involved in the regulation of mitotic spindle dynamics and cell division (11–14). The GTPase-activating protein RGS14 also translocates between the nucleus and the cytoplasm and is associated with centrosomes influencing mitosis (15). Another RGS protein, RGS7, interacts with $G\beta_5$ and migrates into the nucleus as an RGS7-$G\beta_5$ complex (16). Furthermore, signal alteration by G-protein and their various types of regulators is involved in adaptation of cells to maintain homeostasis under pathologic conditions (17–21). In fact, the expression of such regulatory proteins is altered with the development of cardiac hypertrophy in hypertension or in response to pressure overload stress (22, 23).

As part of a broader approach to identify adaptation-specific regulatory proteins for heterotrimeric G-proteins, we previously identified AGS8 from a cDNA library of rat hearts subjected to repetitive transient ischemia (18). AGS8 was up-regulated in cardiomyocytes in response to transient hypoxia and regulated $G\beta\gamma$ signaling. Indeed, AGS8 played a key role in apoptosis of cardiomyocytes induced by hypoxic stress via $G\beta\gamma$ and the channel protein connexin 43 (24). These findings prompted us to investigate the presence of putative AGS proteins in other models of cardiovascular diseases.

We first screened for regulatory proteins for heterotrimeric G-proteins involved in the development of cardiac

* This work was supported, in whole or in part, by National Institutes of Health Grants NS24821 and DA025896 (both to S. M. L.). This work was also supported by Grants-in-aid for Scientific Research (C) 18599006 and 20590212, the Yokohama Foundation for Advancement of Medical Science, and Strategic Research Project Grants K18017 and K19021 from Yokohama City University, Japan (all to M. S.) and by grants from the Ministry of Health Labor and Welfare; Ministry of Education, Culture, Sports, Science and Technology of Japan; Takeda Science Foundation; Cosmetology Research Foundation; and Kitsuen Research Foundation (all to Y. I.).

[S] The on-line version of this article (available at http://www.jbc.org) contains supplemental Figs. 1 and 2 and Text 1–3.

[1] Supported by the Takeda Science Foundation, the NOVARTIS Foundation (Japan) for the Promotion of Science, the Mitsubishi Pharma Research Foundation, The Ichiro Kanehara Foundation, and the Mochida Memorial Foundation for Medical and Pharmaceutical Research. To whom correspondence may be addressed: Cardiovascular Research Inst., Yokohama City University School of Medicine, 3-9 Fukuura, Kanazawa-Ku, Yokohama 236-0004, Japan. Fax: 81-45-788-1470; E-mail: motosato@yokohama-cu.ac.jp.

[2] To whom correspondence may be addressed. E-mail: yishikaw@med.yokohama-cu.ac.jp.

[3] The abbreviations used are: GPCR, G-protein coupled receptor; TFE, transcription factor E; MITF, microphthalmia-associated transcription factor; TFEB, transcription factor EB; AGS, activators of G-protein signaling; RGS, regulator of G protein signaling; TAC, transverse aortic constriction; PLC, phospholipase C.

hypertrophy. Cardiac hypertrophy is a gateway to cardiac dysfunction and acts as an independent risk factor for cardiovascular events. GPCR-mediated signaling pathways, in particular those involving β-adrenergic or angiotensin II receptors, influence gene expression involved in cardiac hypertrophy. Overexpression of $G\alpha_s$ or $G\alpha_q$ in the mouse heart actually results in the development of cardiac hypertrophy and dysfunction.

We report the identification of three $G\alpha_{16}$-selective AGS proteins using a yeast-based discovery platform for receptor-independent activators of G-protein signaling to screen cDNA libraries from mouse models of cardiac hypertrophy induced by transverse aortic constriction (TAC) or continuous infusion of the β-adrenergic agonist isoproterenol. Of importance, the three new AGS proteins are microphthalmia-associated transcription factor (MITF)/TFE transcription factors. Although increased expression of TFE3 in heterologous systems had no influence on receptor-mediated $G\alpha_{16}$ signaling at the plasma membrane, TFE3 actually translocated $G\alpha_{16}$ to the nucleus, leading to the induction of claudin 14, a key component of membrane structure in cardiomyocytes. These findings indicate that $G\alpha_{16}$-selective AGS proteins are up-regulated under pathologic conditions and are involved in a novel mechanism of transcriptional regulation via the relocalization and activation of $G\alpha_{16}$.

EXPERIMENTAL PROCEDURES

Materials

Anti-$G\alpha_{i3}$, anti-$G\alpha_s$, and anti-phospholipase C (PLC)-β2 antibodies and anti-β_2-adrenergic receptor were purchased from Santa Cruz Biotechnology. IGEPAL CA-630 and anti-β-actin antibody were obtained from Sigma. Anti-$G\alpha_{16}$ and anti-claudin 14 antibodies were purchased from Medical and Biological Laboratories, Co., Ltd. (Nagoya, Japan) and Abcam, respectively. Anti-Xpress antibody and Lipofectamine 2000 reagent were obtained from Invitrogen. pcDNA3.1::$G\alpha_{16}$ and pcDNA3.1::$G\alpha_{16}$Q212L were obtained from the Missouri S&T cDNA Resource Center. $G\alpha_{16}$G211A was generated by site-direct mutagenesis (PrimeSTAR Mutagenesis Basal kit, Takara, Otsu, Japan). Full-length mouse TFE3, human transcription factor EB (TFEB), and mouse MITF were subcloned into the pYES2 vector (Invitrogen) or pcDNAHis vector (Invitrogen) from cDNA clones (Open Biosystems) (TFE3, MMM1013-98478992; TFEB, MHS1010-7508073; MITF, EMM1002-97035453).

Animal Models

All animal experiments were performed according to procedures approved by the Institutional Animal Care and Use Committee at Yokohama City University.

TAC—Constriction of the transverse thoracic aorta was performed on 14 male mice (C57BL/6; age, 14–17 weeks; 24–29 g; Charles River Laboratories, Gilroy, CA) as described previously (25). In brief, mice were anesthetized, intubated, and placed on a respirator. The transverse aorta was visualized following midline sternotomy. A 5-0 nylon suture was placed around the aorta distal to the brachiocephalic artery. The suture was tightened around a blunt 27-gauge needle placed adjacent to the aorta to produce −70% constriction. The needle was then removed, and the chest and overlying skin were closed. Six age-matched animals underwent the same surgical procedure but without TAC (sham). Seven days after surgery, the mice were sacrificed for tissue extraction. The left ventricles were quickly separated, frozen in liquid nitrogen, and stored at −70 °C until use.

Cardiac Hypertrophy and Tachycardia—Nineteen male mice (C57BL/6; age, 16–19 weeks; 25–30 g; Charles River Laboratories) were anesthetized, and an osmotic minipump (model 2002, ALZET Osmotic Pumps, Cupertino, CA) was implanted subcutaneously (18). After 7 days of continuous infusion of isoproterenol (60 μg/g of body weight/day), mice were anesthetized, and the hearts were rapidly excised. The left ventricles were rapidly frozen in liquid nitrogen and stored at −70 °C until use.

Generation of cDNA Libraries and Functional Screen in Saccharomyces cerevisiae

mRNA isolated from the left ventricle in the TAC or tachycardia models was used to synthesize cDNAs using a cDNA Synthesis kit (Takara); cDNAs were cloned into the pYES2 yeast expression vector. The cDNA library from the TAC model contained 1.1×10^6 cfu with an average insert size of 1.5 kb, and the library from tachycardia model contained 2.8×10^6 cfu with an average insert size of 1.2 kb. Functional screens and growth assays in the modified strains of *S. cerevisiae* were conducted as described previously (26–28).

Quantitative Polymerase Chain Reaction (PCR)

RNA isolation, cDNA synthesis, and real time PCR analysis were performed as described previously (24). The primers for RT-PCR were as follows: mouse MITF: forward, 5′-ACTTTCCCTTATCCCATCCACC-3′; reverse, 5′-TGAGATCCAGAGTTGTCGTACA-3′; mouse TFE3: forward, 5′-TGCGTCAGCAGCTTATGAGG-3′; reverse, 5′-AGACACGCCAATCACAGAGAT-3′; mouse TFEB: forward, 5′-CCACCCCAGCCATCAACAC-3′; reverse, 5′-CAGACAGATACTCCCGAACCTT-3′; mouse GNA15: forward, 5′-CGCCAGAATCGACCAGGAG-3′; reverse, 5′-GTAGCCCACACCGTGAATGA-3′; mouse claudin 14: forward, 5′-GCATGGTGGGAACGCTCAT-3′; reverse, 5′-CCACAGTCCCTTCAGGTAGGA-3′; human claudin 14: forward, 5′-CAAACACCGCACCTGCCTA-3′; reverse, 5′-CACGTAGTCGTTCAGCCTGT-3′; rat GNA15: forward, 5′-CAGGAGAACCGTATGAAGGAGAGTC-3′; reverse, 5′-CAGGATGTCTGTCTTGTTGAGGAAG-3′; rat TFE3: forward, 5′-TGTTCGTGCTGTTGGAAGAGC-3′; reverse, 5′-GGGATAGAGGCTGGCTTTTGAG-3′; rat claudin 14: forward, 5′-TCATCACTACTATCCTGCCGCAC-3′; reverse, 5′-ACACACTCCATCCACAGTCCCTTC-3′; and 18 S: forward, 5′-GTAACCCGTTGAACCCCATT-3′; reverse, 5′-CCATCCAATCGGTAGTAGCG-3′. All PCRs were performed in duplicate or triplicate at 95 °C for 2 min followed by 40 cycles at 95 °C for 30 s and 60 or 62 °C for 45 s. The cycle threshold values corresponding to the PCR cycle number at which fluorescence emission in real time reaches a threshold above the base-line emission were determined. 18 S ribosomal